2011-02

Computing K and D meson masses with twisted mass lattice QCD

Baron, R

10.1016/j.cpc.2010.10.004
Computer Physics Communications
Elsevier BV

Computing K and D meson masses with $N_{\rm f} = 2 + 1 + 1$ twisted mass lattice QCD

SFB/CPP-09-31, LPSC1049, MS-TP-10-10, DESY 10-055, LTH874, LPT-Orsay 10-30, HU-EP-10/19

Remi Baron[a], **Philippe Boucaud**[b], **Jaume Carbonell**[c], **Vincent Drach**[c], **Federico Farchioni**[d], **Gregorio Herdoiza**[e], **Karl Jansen**[e], **Chris Michael**[f], **Istvan Montvay**[g], **Elisabetta Pallante**[h], **Olivier Pène**[b], **Siebren Reker**[h], **Carsten Urbach**[i], **Marc Wagner**[j], **Urs Wenger**[k]

[a] CEA, Centre de Saclay, IRFU/Service de Physique Nucléaire, F-91191 Gif-sur-Yvette, France
[b] Laboratoire de Physique Théorique (Bât. 210), CNRS et Université Paris-Sud XI, Centre d'Orsay, 91405 Orsay-Cedex, France
[c] Laboratoire de Physique Subatomique et Cosmologie, 53 avenue des Martyrs, 38026 Grenoble, France
[d] Universität Münster, Institut für Theoretische Physik, Wilhelm-Klemm-Straße 9, D-48149 Münster, Germany
[e] NIC, DESY, Platanenallee 6, D-15738 Zeuthen, Germany
[f] Division of Theoretical Physics, University of Liverpool, L69 3BX Liverpool, United Kingdom
[g] Deutsches Elektronen-Synchrotron DESY, Notkestr. 85, D-22603 Hamburg, Germany
[h] Centre for Theoretical Physics, University of Groningen, Nijenborgh 4, 9747 AG Groningen, the Netherlands
[i] Helmholtz-Institut für Strahlen- und Kernphysik (Theorie) and Bethe Center for Theoretical Physics, Universität Bonn, 53115 Bonn, Germany
[j] Humboldt-Universität zu Berlin, Institut für Physik, Newtonstraße 15, D-12489 Berlin, Germany
[k] Albert Einstein Center for Fundamental Physics, Institute for Theoretical Physics, University of Bern, Sidlerstr. 5, CH-3012 Bern, Switzerland

May 12, 2010

Abstract

We discuss the computation of the mass of the K and D mesons within the framework of $N_{\rm f} = 2 + 1 + 1$ twisted mass lattice QCD from a technical point of view. These quantities are essential, already at the level of generating gauge configurations, being obvious candidates to tune the strange and charm quark masses to their physical values. In particular, we address the problems related to the twisted mass flavor and parity symmetry breaking, which arise when considering a non-degenerate (c, s) doublet. We propose and verify the consistency of three methods to extract the K and D meson masses in this framework.

1 Introduction

The framework of maximally twisted mass fermions as an $\mathcal{O}(a)$ improved lattice formulation [47] has been proved to be highly successful in recent years. The European Twisted Mass Collaboration (ETMC) has adopted this formulation and has carried through a broad research program with $N_{\rm f} = 2$ flavors of mass-degenerate quarks in various areas of lattice QCD including light meson physics [1, 2, 3], spectroscopy of light baryons [4, 5], strange and charm physics [6, 7, 8], B-physics [9, 10], spectroscopy of static-light mesons [11, 12], Isgur-Wise functions [13], meson [14, 15, 16] and nucleon [17] form factors, moments of parton distribution functions [18], neutral [19] and η' [20] mesons, $\omega - \rho$ mass splitting [21], the vacuum polarization tensor [22], pion scattering lengths [23], an investigation of the ρ meson as a resonance [24] or the non-perturbative renormalization of quark bilinear operators [25].

Particular emphasis has been laid on the cut-off effects appearing at $\mathcal{O}(a^2)$ in the twisted mass formulation at maximal twist. These effects have been studied theoretically at tree-level of perturbation theory [26], and within the Symanzik approach [32, 33]. These analyses suggest that isospin breaking effects strongly affect only a limited set of observables, namely the neutral pion mass and kinematically related quantities [33]. The same effects have been numerically investigated in the quenched approximation [27, 28, 29], with two dynamical flavors [3, 4, 5, 30, 31] and with $N_{\rm f} = 2 + 1 + 1$ [38]. All numerical results up to date are in agreement with the theoretical conclusions.

The studies collected so far suggest that the twisted mass formulation at maximal twist is a viable realization of QCD on the lattice, with the major advantage of automatic $\mathcal{O}(a)$ improvement of physical observables, independently of the specific type of operator considered. Other advantages worth to mention are that the twisted mass term acts as an infrared regulator of the theory and that mixing patterns in the renormalisation procedure are expected to be simplified. It is hence natural to go one step further and include dynamical strange and charm quarks in the simulations. The theoretical ground for this has been provided in ref. [34] and first feasibility studies have been performed in ref. [35]. In the last years, we have initiated a comprehensive research program with dynamical $N_{\rm f} = 2 + 1 + 1$ flavors of quarks. Encouraging preliminary results were reported in [36, 37], while a companion paper [38] presents a more detailed analysis of the light meson sector for the ensembles used in this paper.

A difficulty arises in $N_{\rm f} = 2+1+1$ maximally twisted mass lattice QCD when adding a strange and a charm quark, due to the explicit violation of the strange and charm flavor quantum number conservation. At any non-vanishing value of the lattice spacing, the latter leads to the contamination of correlators by unphysical contributions from intermediate states carrying the wrong quantum numbers. Moreover, transitions that are not allowed in continuum QCD become possible, the consequence being that stable states in the continuum with respect to strong interactions, such as the D meson, become resonances.

In this paper, we provide algorithmic and methodological tools to tackle the problem. In particular, we present three techniques, a generalized eigenvalue problem, multiple exponential fits, and enforcing parity and flavor symmetry restoration, to compute the physical K and D meson masses. As we will demonstrate below, we find that with all three methods these masses can be extracted and results agree among the three methods. The paper is conceived as a technical report on these methods, which can in general be applied whenever flavor symmetry breaking occurs. Efforts to implement these techniques in combination with a flavor diagonal

Osterwalder-Seiler valence quark action, see e.g. [6, 34, 42, 43], are ongoing.

The paper is organized as follows. In section 2 we define the setup, the operators used, and the optimization of the correlation matrices. Section 3 describes the determination of the K and D meson masses with the three methods. We conclude in section 4.

2 Simulation setup

2.1 $N_{\rm f} = 2+1+1$ twisted mass lattice QCD

This work is based on sets of configurations generated by the ETM collaboration [36, 37] with the Iwasaki gauge action [44] and $N_{\rm f} = 2+1+1$ flavors of twisted mass quarks. The light degenerate (u,d) quark doublet is described by the standard twisted mass action [45]

$$S_{\rm F,light}[\chi^{(l)},\bar{\chi}^{(l)},U] \;=\; a^4\sum_x \bar{\chi}^{(l)}(x)\Big(D_{\rm W}(m_0)+i\mu\gamma_5\tau_3\Big)\chi^{(l)}(x), \tag{1}$$

while for the (c,s) doublet the twisted mass formulation for non-degenerate quarks of [46] has been used:

$$S_{\rm F,heavy}[\chi^{(h)},\bar{\chi}^{(h)},U] \;=\; a^4\sum_x \bar{\chi}^{(h)}(x)\Big(D_{\rm W}(m_0)+i\mu_\sigma\gamma_5\tau_1+\tau_3\mu_\delta\Big)\chi^{(h)}(x). \tag{2}$$

In both cases $D_{\rm W}$ denotes the standard Wilson Dirac operator

$$D_{\rm W}(m_0) \;=\; \frac{1}{2}\Big(\gamma_\mu\Big(\nabla_\mu+\nabla^*_\mu\Big)-a\nabla^*_\mu\nabla_\mu\Big)+m_0, \tag{3}$$

while $\chi^{(l)}=(\chi^{(u)},\chi^{(d)})$ and $\chi^{(h)}=(\chi^{(c)},\chi^{(s)})$ are the quark fields in the so-called twisted basis. For reasons explained in [35] the same value of the standard quark mass parameter m_0 has been used in both sectors.

When tuning the theory to maximal twist, automatic $\mathcal{O}(a)$ improvement for physical quantities applies [46, 47]. This tuning has been done by adjusting m_0 such that the PCAC quark mass in the light quark sector vanishes [38],

$$am^{\rm PCAC}_{\chi^{(l)}} \;=\; \frac{\sum_{\mathbf{x}}\Big\langle \partial^*_0 A^{(l)+}_0(x)P^{(l)-}(y)\Big\rangle}{2\sum_{\mathbf{x}}\Big\langle P^{(l)+}(x)P^{(l)-}(y)\Big\rangle} \;=\; 0\,, \tag{4}$$

with the bilinears defined as

$$A^{(l)+}_\mu \;=\; \bar{\chi}^{(u)}\gamma_\mu\gamma_5\chi^{(d)} \quad,\quad P^{(l)+} \;=\; \bar{\chi}^{(u)}\gamma_5\chi^{(d)} \quad,\quad P^{(l)-} \;=\; \bar{\chi}^{(d)}\gamma_5\chi^{(u)}. \tag{5}$$

At maximal twist, in a massless quark renormalization scheme, the renormalized quark masses are related to the bare parameters μ_σ and μ_δ by [46]

$$m^R_s \;=\; Z_P^{-1}\Big(\mu_\sigma-\frac{Z_P}{Z_S}\mu_\delta\Big) \qquad,\qquad m^R_c \;=\; Z_P^{-1}\Big(\mu_\sigma+\frac{Z_P}{Z_S}\,,\mu_\delta\Big) \tag{6}$$

where Z_P and Z_S are the renormalization constants of the non-singlet pseudoscalar and scalar densities in a massless quark scheme, namely for $N_{\rm f} = 4$ massless Wilson lattice QCD.

The values of μ_σ and μ_δ have been adjusted in our simulations by requiring that the simulated kaon and D meson mass approximately assume their physical values [38]. For this study we consider two ensembles, one from each of the currently simulated β values, $\beta = 1.90$ and $\beta = 1.95$ [36, 37, 38], with a light pseudoscalar mass $m_{\rm PS} \approx 320\,\text{MeV}$ in both cases, see Table 1.

Ensemble	β	$(L/a)^3 \times T/a$	$a\mu$	κ	$a\mu_\sigma$	$a\mu_\delta$	a in fm	$m_{\rm PS}$ in MeV	# of gauges
A40.32	1.90	$32^3 \times 64$	0.0040	0.163270	0.150	0.190	0.086	324	1003
B35.32	1.95	$32^3 \times 64$	0.0035	0.161240	0.135	0.170	0.078	318	1042

Table 1: Summary of the ensembles considered in this paper, more details in [36, 37, 38].

2.2 Meson creation operators and trial states

2.2.1 Quantum numbers, physical basis and twisted basis

We are concerned with computing the mass of the K meson, m_K, and of the D meson, m_D, within the setup defined by eqs. (1) to (3). Both mesons have total angular momentum $J = 0$ and parity $\mathcal{P} = -$. Their quark content is e.g. $\bar{K}^0 \equiv \bar{d}s$ and $D^+ \equiv \bar{d}c$.

Neither heavy flavor nor parity are exact symmetries in $N_{\rm f} = 2+1+1$ twisted mass lattice QCD at finite lattice spacing. In particular, the τ_1-coupling term in eq. (2) violates the conservation of the strange and charm flavor quantum numbers. Consequently, instead of four different heavy-light meson sectors $(s,-)$, $(s,+)$, $(c,-)$ and $(c,+)$ there is only a single mixed flavor-parity sector $(s/c,-/+)$. Problems arise in particular when one tries to determine m_D. In continuum QCD the D meson is the lowest state in the $(c,-)$ sector, while in our setup it is a highly excited state in the combined sector $(s/c,-/+)$. Notice that, besides the K meson, there are a radially excited K state ($K(1460)$), possibly strange mesons with positive parity ($K_0^*(800)$, $K_0^*(1430)$) and a number of multi particle states $K/K_0^* + n \times \pi$ [48]. Hence, for a clean extraction of m_D one has to consider sufficiently large correlation matrices, which are able to resolve all these low lying states. This is possible in principle. In practice, the separation of the excited states would require the determination of correlation matrices with extremely high statistical precision. At our currently available statistics, this route seems not to be viable.

Our approach is instead based on the observation that parity and heavy flavor symmetries are restored in the continuum limit, where the twisted mass theory is expected to reproduce QCD with $N_{\rm f} = 2 + 1 + 1$ quark flavors. In this limit, operators with definite parity [47] and flavor quantum numbers projecting onto the physical meson states can be reconstructed (cf. section 3.3). As it is shown in the following, these operators can be defined as linear combinations of bilinears of the lattice quark fields in the twisted basis.

In the continuum, or in any chirality preserving lattice formulation [45], the twist transformation

relating the physical quark fields ψ and the twisted quark fields χ reads

$$\psi^{(l)} = e^{i\omega_l\gamma_5\tau_3/2}\chi^{(l)} \quad , \quad \bar{\psi}^{(l)} = \bar{\chi}^{(l)}e^{i\omega_l\gamma_5\tau_3/2} \tag{7}$$

$$\psi^{(h)} = e^{i\omega_h\gamma_5\tau_1/2}\chi^{(h)} \quad , \quad \bar{\psi}^{(h)} = \bar{\chi}^{(h)}e^{i\omega_h\gamma_5\tau_1/2}, \tag{8}$$

where $\omega_{l,h}$ are the twist angles in the light and heavy quark sector, respectively. Analogous relations hold for operators projecting, in the continuum limit, on trial states with definite heavy flavor and parity quantum numbers. In the physical basis, such operators can be chosen according to[1]

$$\mathcal{O}_{\rm ph} = \begin{pmatrix} \mathcal{O}_{\rm ph}^{(s,\gamma_5)} \\ \mathcal{O}_{\rm ph}^{(c,\gamma_5)} \\ \mathcal{O}_{\rm ph}^{(s,1)} \\ \mathcal{O}_{\rm ph}^{(c,1)} \end{pmatrix} = \begin{pmatrix} +i\bar{\psi}^{(d)}\gamma_5\psi^{(s)} \\ -i\bar{\psi}^{(d)}\gamma_5\psi^{(c)} \\ +\bar{\psi}^{(d)}\psi^{(s)} \\ -\bar{\psi}^{(d)}\psi^{(c)} \end{pmatrix} \tag{9}$$

The twist rotations in eqs. (7) and (8) relate the twisted basis operators

$$\mathcal{O}_{\chi} = \begin{pmatrix} \mathcal{O}_{\chi}^{(s,\gamma_5)} \\ \mathcal{O}_{\chi}^{(c,\gamma_5)} \\ \mathcal{O}_{\chi}^{(s,1)} \\ \mathcal{O}_{\chi}^{(c,1)} \end{pmatrix} = \begin{pmatrix} +i\bar{\chi}^{(d)}\gamma_5\chi^{(s)} \\ -i\bar{\chi}^{(d)}\gamma_5\chi^{(c)} \\ +\bar{\chi}^{(d)}\chi^{(s)} \\ -\bar{\chi}^{(d)}\chi^{(c)} \end{pmatrix} \tag{10}$$

to the physical operators of eq. (9) as follows

$$\mathcal{O}_{\rm ph} = \mathcal{M}(\omega_l,\omega_h)\,\mathcal{O}_{\chi} \quad , \quad \mathcal{O}_{\rm ph}^{\dagger} = \mathcal{O}_{\chi}^{\dagger}\,\mathcal{M}^T(\omega_l,\omega_h)\,, \tag{11}$$

with the orthogonal twist rotation matrix given by

$$\mathcal{M}(\omega_l,\omega_h) = \begin{pmatrix} \cos\frac{\omega_l}{2}\cos\frac{\omega_h}{2} & -\sin\frac{\omega_l}{2}\sin\frac{\omega_h}{2} & -\sin\frac{\omega_l}{2}\cos\frac{\omega_h}{2} & -\cos\frac{\omega_l}{2}\sin\frac{\omega_h}{2} \\ -\sin\frac{\omega_l}{2}\sin\frac{\omega_h}{2} & \cos\frac{\omega_l}{2}\cos\frac{\omega_h}{2} & -\cos\frac{\omega_l}{2}\sin\frac{\omega_h}{2} & -\sin\frac{\omega_l}{2}\cos\frac{\omega_h}{2} \\ \sin\frac{\omega_l}{2}\cos\frac{\omega_h}{2} & \cos\frac{\omega_l}{2}\sin\frac{\omega_h}{2} & \cos\frac{\omega_l}{2}\cos\frac{\omega_h}{2} & -\sin\frac{\omega_l}{2}\sin\frac{\omega_h}{2} \\ \cos\frac{\omega_l}{2}\sin\frac{\omega_h}{2} & \sin\frac{\omega_l}{2}\cos\frac{\omega_h}{2} & -\sin\frac{\omega_l}{2}\sin\frac{\omega_h}{2} & \cos\frac{\omega_l}{2}\cos\frac{\omega_h}{2} \end{pmatrix}. \tag{12}$$

However, when using the Wilson lattice formulation, the operators in eq. (10), with and without a γ_5 matrix, renormalize differently due to the explicit breaking of chiral symmetry. This implies that, to be able to build a representation of the chiral group, renormalization factors must explicitly be taken into account, and eq. (11) only holds for the renormalized counterparts

$$\mathcal{O}_{\rm ph}^{R} = \mathcal{M}(\omega_l,\omega_h)\,\mathcal{O}_{\chi}^{R} \quad , \quad (\mathcal{O}_{\rm ph}^{R})^{\dagger} = (\mathcal{O}_{\chi}^{R})^{\dagger}\,\mathcal{M}^T(\omega_l,\omega_h), \tag{13}$$

where the bilinears in eq. (10) have been replaced by their renormalized versions,

$$\mathcal{O}_{\chi}^{R} = {\rm diag}\Big(Z_P, Z_P, Z_S, Z_S\Big)\,\mathcal{O}_{\chi} = \begin{pmatrix} Z_P\,\mathcal{O}_{\chi}^{(s,\gamma_5)} \\ Z_P\,\mathcal{O}_{\chi}^{(c,\gamma_5)} \\ Z_S\,\mathcal{O}_{\chi}^{(s,1)} \\ Z_S\,\mathcal{O}_{\chi}^{(c,1)} \end{pmatrix}, \tag{14}$$

[1]For definiteness we identify the light flavor with d.

and Z_P and Z_S are the same renormalization factors as in (6). At maximal twist, i.e. $\omega_l = \omega_h = \pi/2$, one has

$$\begin{pmatrix} \mathcal{O}^{(s,\gamma_5)}_{\rm ph} \\ \mathcal{O}^{(c,\gamma_5)}_{\rm ph} \\ \mathcal{O}^{(s,1)}_{\rm ph} \\ \mathcal{O}^{(c,1)}_{\rm ph} \end{pmatrix}^R = \frac{1}{2} \begin{pmatrix} 1 & -1 & -1 & -1 \\ -1 & 1 & -1 & -1 \\ 1 & 1 & 1 & -1 \\ 1 & 1 & -1 & 1 \end{pmatrix} \begin{pmatrix} Z_P\, \mathcal{O}^{(s,\gamma_5)}_{\chi} \\ Z_P\, \mathcal{O}^{(c,\gamma_5)}_{\chi} \\ Z_S\, \mathcal{O}^{(s,1)}_{\chi} \\ Z_S\, \mathcal{O}^{(c,1)}_{\chi} \end{pmatrix} . \tag{15}$$

A third definition of the quark fields will be useful in the following (where maximal twist applies), obtained by rotating the lattice χ-fields via eqs. (7) and (8), where now $\omega_l = \omega_h = \pi/2$. The rotated fields would reproduce the physical ones in a theory with exact chiral symmetry and $Z_P = Z_S$. In the present formulation with broken chiral symmetry, they define instead a "pseudo physical basis" (ppb). We denote the rotated fields with $\psi^{(l,\,h)}_{\rm ppb}$ and introduce the operator bilinears in this basis

$$\mathcal{O}_{\rm ppb} = \begin{pmatrix} \mathcal{O}^{(s,\gamma_5)}_{\rm ppb} \\ \mathcal{O}^{(c,\gamma_5)}_{\rm ppb} \\ \mathcal{O}^{(s,1)}_{\rm ppb} \\ \mathcal{O}^{(c,1)}_{\rm ppb} \end{pmatrix} = \begin{pmatrix} +i\bar{\psi}^{(d)}_{\rm ppb}\gamma_5\psi^{(s)}_{\rm ppb} \\ -i\bar{\psi}^{(d)}_{\rm ppb}\gamma_5\psi^{(c)}_{\rm ppb} \\ +\bar{\psi}^{(d)}_{\rm ppb}\psi^{(s)}_{\rm ppb} \\ -\bar{\psi}^{(d)}_{\rm ppb}\psi^{(c)}_{\rm ppb} \end{pmatrix} = \frac{1}{2} \begin{pmatrix} 1 & -1 & -1 & -1 \\ -1 & 1 & -1 & -1 \\ 1 & 1 & 1 & -1 \\ 1 & 1 & -1 & 1 \end{pmatrix} \begin{pmatrix} \mathcal{O}^{(s,\gamma_5)}_{\chi} \\ \mathcal{O}^{(c,\gamma_5)}_{\chi} \\ \mathcal{O}^{(s,1)}_{\chi} \\ \mathcal{O}^{(c,1)}_{\chi} \end{pmatrix} , \tag{16}$$

otherwise written as

$$\mathcal{O}_{\rm ppb} = \mathcal{M}(\pi/2, \pi/2)\, \mathcal{O}_{\chi} \equiv \mathcal{M}_{\rm mt}\, \mathcal{O}_{\chi} . \tag{17}$$

The physical operators defined in eq. (13), and eq. (15) at maximal twist, project onto states that converge to states with definite flavor and parity quantum numbers in the continuum limit. Since we aim to determine the ground states of the physical system, in at least two of the four sectors, it is appropriate to first build the correlation matrices in terms of the building blocks given in eq. (10). We also project to zero momentum by summing over all lattice sites at fixed Euclidean time t,

$$\mathcal{O}^{(h,\Gamma)}_{\chi}(t) = \eta_\Gamma \sum_{\mathbf{x}} \bar{\chi}^{(d)}(\mathbf{x},t)\Gamma\chi^{(h)}(\mathbf{x},t) \ , \ h \in \{s\,,\,c\} \ , \ \Gamma \in \{\gamma_5\,,\,1\} \ \ (\eta_1 = \pm 1, \eta_{\gamma_5} = \pm i) \ . \tag{18}$$

The corresponding trial states

$$|\phi^{(h,\Gamma)}_{\chi}(t)\rangle = \Big(\mathcal{O}^{(h,\Gamma)}_{\chi}(t)\Big)^\dagger |\Omega\rangle \tag{19}$$

enter the correlation matrices

$$C_{(h_2,\Gamma_2),(h_1\Gamma_1)}(t_2 - t_1) = \langle \phi^{(h_2,\Gamma_2)}_{\chi}(t_2) | \phi^{(h_1,\Gamma_1)}_{\chi}(t_1)\rangle = \langle\Omega| \Big(\mathcal{O}^{(h_2,\Gamma_2)}_{\chi}(t_2)\Big)\Big(\mathcal{O}^{(h_1,\Gamma_1)}_{\chi}(t_1)\Big)^\dagger |\Omega\rangle \ , \tag{20}$$

and we introduce the shorthand matrix notation for later use

$$C(t_2 - t_1) = \Big\langle \mathcal{O}(t_2) \otimes (\mathcal{O}(t_1))^\dagger \Big\rangle \ . \tag{21}$$

Notice also that, due to the discrete symmetries of the twisted mass action in eqs. (1) and (2), the correlation $C(t_2 - t_1)$ is a real and symmetric matrix. Eqs. (18) to (21) can also be generalized to the case of more operators, as for example operators with different levels of smearing (see the next section) or Dirac structure. In this case $C(t_2-t_1)$ will be a $D \times D$ matrix ($D = 4 \times n$) defined by the larger operator set. An application of this kind will be considered in section 3.2. One can easily obtain another set of independent meson creation operators with identical quantum numbers by replacing $\Gamma \to \gamma_0\Gamma$. We found, however, that the corresponding trial states have worse overlaps to the low lying states of interest. Therefore, we do not consider these operators in the following. To improve the signal-to-noise ratio, we have computed the correlators in eq. (20) by using the one-end trick [1, 2].

2.2.2 Operator optimization by means of smearing

To optimize the overlap of the trial states in eq. (19) with the physical K and D mesons, we resort to standard smearing techniques. We use Gaussian smeared quark fields, with APE smeared spatial links. Additional details can be found in [11], where the same setup has been used.

We have optimized the smearing by computing effective masses at $t = 1$ and $t_0 = 1$ (cf. (25)), where excited states are suppressed the least, for different values of $N_{\rm Gauss}$, and $\kappa_{\rm Gauss} = 0.5$, $N_{\rm APE} = 10$, $\alpha_{\rm APE} = 0.5$ kept fixed. This optimization is essentially independent on the lattice volume and on the light quark mass. Results for $\beta = 3.90$, $L^3 \times T = 24^3 \times 48$ and $\mu = 0.0040$ are reported in Figure 1. Although the suppression of excited states only weakly depends on $N_{\rm Gauss}$ and, therefore, on the width of the corresponding trial states, it is obvious that the D meson has a somewhat smaller width than the K meson. Since the D meson is heavier and hence more difficult to compute, we focus on optimizing the overlap with the D meson state and choose $N_{\rm Gauss} = 30$. An estimate of the corresponding trial state radius R can be obtained via [11]

$$\frac{R}{a} \;=\; \left(\frac{N_{\rm Gauss}\kappa_{\rm Gauss}}{1+6\kappa_{\rm Gauss}}\right)^{1/2}, \tag{22}$$

yielding $R_K \approx 7a \approx 0.60\,\mathrm{fm}$ and $R_D \approx 5a \approx 0.43\,\mathrm{fm}$ (cf. Figure 1b). A similar optimization for the parameter $N_{\rm APE}$ shows essentially no dependence on the ground state overlap. This is exemplified in Figure 2 corresponding to $\beta = 3.90$, $L^3 \times T = 24^3 \times 48$ and $\mu = 0.0100$.

We end up with the following optimized set of smearing parameters for ensemble A40.32:

$$N_{\rm Gauss} = 30 \quad , \quad \kappa_{\rm Gauss} = 0.5 \quad , \quad N_{\rm APE} = 10 \quad , \quad \alpha_{\rm APE} = 0.5. \tag{23}$$

Given the rather mild dependence of the ground state overlap on $N_{\rm Gauss}$ and $N_{\rm APE}$, we use the set of parameters in eq. (23) also for the ensemble B35.32, with only slightly different lattice spacing. Sometimes in the following of this paper, we will also consider correlation matrices made of local operators, or mixed local and smeared operators. However, the final determination of all masses will exclusively be obtained with the correlation matrix made of the smeared operators, with the optimized smearing parameters of eq. (23).

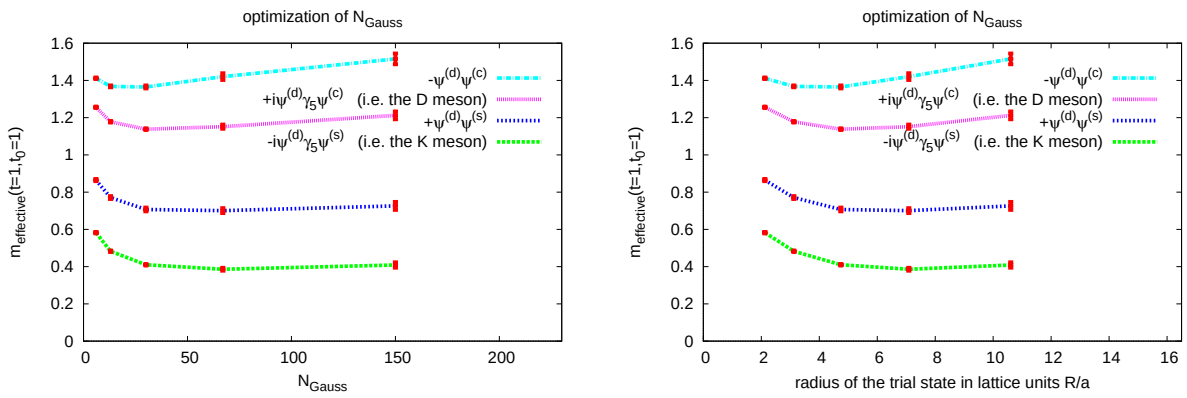

Figure 1: **a)** The effective masses $m^{(n)}_{\text{effective}}(t = 1, t_0 = 1)$ (cf. eq. (25)) for the trial states defined in eq. (19) as functions of N_{Gauss} for $\beta = 3.90$, $L^3 \times T = 24^3 \times 48$ and $\mu = 0.0040$ with $\kappa_{\text{Gauss}} = 0.5$, $N_{\text{APE}} = 10$, $\alpha_{\text{APE}} = 0.5$. **b)** The same effective masses as a function of the radius of the trial states in lattice units R/a with $\kappa_{\text{Gauss}} = 0.5$.

3 Computation of m_K and m_D

In contrast to parity and flavor conserving lattice formulations, as the standard Wilson lattice QCD, it is not possible to compute correlation functions restricted to a single parity and heavy flavor sector in our $N_{\text{f}} = 2 + 1 + 1$ twisted mass framework, as outlined in section 2.2.1. While the determination of m_K is anyway straightforward, since the kaon is the lowest state in the combined heavy flavor and parity sector, the extraction of m_D remains rather problematic, being the D meson a highly excited state. Besides computing m_K with high precision, we attempt in the following to estimate m_D without computing the full low-lying spectrum. We present and compare three different methods, all based on the fact that both heavy flavor symmetry and parity are only weakly broken, by terms of $\mathcal{O}(a)$. The three methods yield a consistent picture.

3.1 Method 1: solving a generalized eigenvalue problem

We consider 4×4 correlation matrices, as defined in eq. (20), computed with the twisted basis operators of eq. (10) and the optimized smearing parameters given in eq. (23). We then solve the generalized eigenvalue problem

$$\sum_k C_{jk}(t) v^{(n)}_k(t, t_0) \quad = \quad \sum_k C_{jk}(t_0) v^{(n)}_k(t, t_0) \lambda^{(n)}(t, t_0) \quad , \quad t \quad \equiv \quad t_2 - t_1 \tag{24}$$

where k runs over the set (h, Γ), $h = c, s$, $\Gamma = \pm$, and obtain the four effective masses $m^{(n)}_{\text{effective}}$, with $n = 0, \ldots, 3$, by solving [49]

$$\frac{\lambda^{(n)}(t, t_0)}{\lambda^{(n)}(t + 1, t_0)} \quad = \quad \frac{e^{-m^{(n)}_{\text{effective}}(t,t_0)t} + e^{-m^{(n)}_{\text{effective}}(t,t_0)(T-t)}}{e^{-m^{(n)}_{\text{effective}}(t,t_0)(t+1)} + e^{-m^{(n)}_{\text{effective}}(t,t_0)(T-(t+1))}} , \tag{25}$$

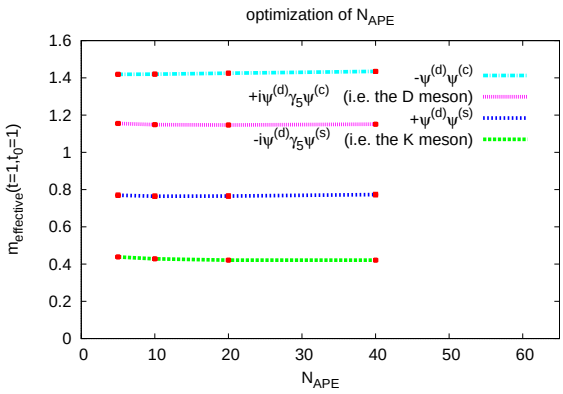

Figure 2: The effective masses $m^{(n)}_{\text{effective}}(t=1,t_0=1)$ as in Figure 1, as a function of N_{APE} for $\beta = 3.90$, $L^3 \times T = 24^3 \times 48$ and $\mu = 0.0100$ with $\alpha_{\text{APE}} = 0.5$, $N_{\text{Gauss}} = 30$, $\kappa_{\text{Gauss}} = 0.5$.

with T the temporal extension of the periodic lattice.

To interpret these effective masses, we assume that heavy flavor and parity breaking effects are small. Indeed they are only $\mathcal{O}(a)$, since they originate from the flavor non-diagonal and parity odd Wilson term, which is proportional to the lattice spacing. Consequently, for vanishing lattice spacing, where heavy flavor and parity are exact symmetries, these correlation matrices would be diagonal in the physical basis, because the operators in eq. (9) would excite orthogonal trial states. Thus, solving the generalized eigenvalue problem as stated in eq. (24) would directly provide the four effective masses with definite heavy flavor and parity. In particular, one of them would have associated quantum numbers $(c, -)$ and would approach a plateau for large temporal separation to be identified with the D meson mass.

At finite lattice spacing in the presence of heavy flavor and parity breaking the four effective masses will approach the masses of the four lowest states in the mixed sector $(s/c, -/+)$ for large temporal separations. The D meson is not among those states: K and K_0^*, the radial excitations and $K/K_0^* + n \times \pi$ states are lighter than the D. At intermediate times, however, one of the four effective masses should still be dominated by the D meson and the corresponding plateau will give a measure of m_D.

To identify the heavy flavor and parity content of the four effective masses, we first note that the trial state corresponding to the n-th effective mass is

$$|\phi^{(n)}_\chi(t)\rangle \quad = \quad \sum_k v^{(n)}_k(t,t_0) \left(\mathcal{O}^{(k)}_\chi(t)\right)^\dagger |\Omega\rangle \ , \tag{26}$$

When the relations $\omega_l = \omega_h = \pi/2$ and $Z_P/Z_S = 1$ are approximately fulfilled, one can rotate to the pseudo physical basis. By inserting eq. (16) into the trial state in (26) and using the orthogonality of the twist rotation matrix $\mathcal{M}_{\text{mt}}$ at maximal twist of eq. (17), yields

$$|\phi^{(n)}_\chi(t)\rangle \quad = \quad \sum_k \left(\mathcal{M}_{\text{mt}}\, v^{(n)}(t,t_0)\right)_k \left(\mathcal{O}^{(k)}_{\text{ppb}}(t)\right)^\dagger |\Omega\rangle \, . \tag{27}$$

By sorting the terms in eq. (27) according to the pseudo physical basis states $(\mathcal{O}^{(k)}_{\rm ppb})^\dagger|\Omega\rangle$, the approximate heavy flavor and parity contents of the trial state corresponding to the n-th effective mass can be read off, and it is given by $c^{(n)}_{(h,\Gamma)} \propto |(\mathcal{M}_{\rm mt}\, v^{(n)}(t,t_0))_{(h,\Gamma)}|^2$. Explicitly,

$$c^{(n)}_{(s,\gamma_5)} = \frac{1}{N}\left| + v^{(n)}_{(s,\gamma_5)} - v^{(n)}_{(c,\gamma_5)} - v^{(n)}_{(s,1)} - v^{(n)}_{(c,1)}\right|^2 \tag{28}$$

$$c^{(n)}_{(c,\gamma_5)} = \frac{1}{N}\left| - v^{(n)}_{(s,\gamma_5)} + v^{(n)}_{(c,\gamma_5)} - v^{(n)}_{(s,1)} - v^{(n)}_{(c,1)}\right|^2 \tag{29}$$

$$c^{(n)}_{(s,1)} = \frac{1}{N}\left| + v^{(n)}_{(s,\gamma_5)} + v^{(n)}_{(c,\gamma_5)} + v^{(n)}_{(s,1)} - v^{(n)}_{(c,1)}\right|^2 \tag{30}$$

$$c^{(n)}_{(c,1)} = \frac{1}{N}\left| + v^{(n)}_{(s,\gamma_5)} + v^{(n)}_{(c,\gamma_5)} - v^{(n)}_{(s,1)} + v^{(n)}_{(c,1)}\right|^2 , \tag{31}$$

where N is a suitable normalization such that

$$c^{(n)}_{(s,\gamma_5)} + c^{(n)}_{(c,\gamma_5)} + c^{(n)}_{(s,1)} + c^{(n)}_{(c,1)} = 1 . \tag{32}$$

To give a specific example, if $c^{(n)}_{(c,\gamma_5)} \simeq 1$, while $c^{(n)}_{(s,\gamma_5)} \simeq c^{(n)}_{(s,1)} \simeq c^{(n)}_{(c,1)} \simeq 0$, the n-th state would be interpreted as the D meson. In the continuum limit, where parity and heavy flavor symmetry are restored, each state will have one associated coefficient $c^{(n)}_{(h,\Gamma)} = 1$, and all others vanishing.

Figure 3 shows the first four effective masses $m^{(n)}_{\rm effective}$ $(n = 0, \ldots, 3)$ as functions of t for the ensembles A40.32 (left) and B35.32 (right), while Figure 4 shows the approximate heavy flavor and parity contents of those states for the ensemble A40.32, measured by the coefficients in eqs. (28) to (31). As expected, each one of the effective masses is strongly dominated by and, therefore, should correspond to one of the sectors $(s,-)$, $(s,+)$, $(c,-)$ and $(c,+)$, which are approximately projected by the pseudo physical basis operators associated to the labels (s,γ_5), $(s,1)$, (c,γ_5) and $(c,1)$, respectively.

To extract the numerical values for m_K and m_D, we perform χ^2 minimizing fits to the corresponding effective mass plateaus. The fitting intervals $[t_{\rm min}, t_{\rm max}]$ are chosen as follows:

- $t_{\rm max} = T/2 - 1 = 31$ for the K meson.
- For all the other states $t_{\rm max}$ is the largest t before which the corresponding effective mass is lost in statistical noise (cf. Table 2).
- $t_{\rm min}$ is the smallest t fulfilling the following two requirements:
  - $t_0 + 1 \leq t_{\rm min} \leq t_{\rm max}$.
  - All fitting intervals $[t_{\rm min}, t'_{\rm max}]$, with $t_{\rm min} + 1 \leq t'_{\rm max} \leq t_{\rm max}$, yield a $\chi^2/{\rm dof} \leq (\chi^2/{\rm dof})_{\rm max}$, and we require $(\chi^2/{\rm dof})_{\rm max} = 2.0$.

  By choosing $t_{\rm min}$ in this way we prevent that effective masses at large t with large statistical errors effectively increase the number of degrees of freedom, while not contributing to the χ^2; in practice, the inclusion of these points would allow to fit ranges with too small values of $t_{\rm min}$, outside the plateau region.

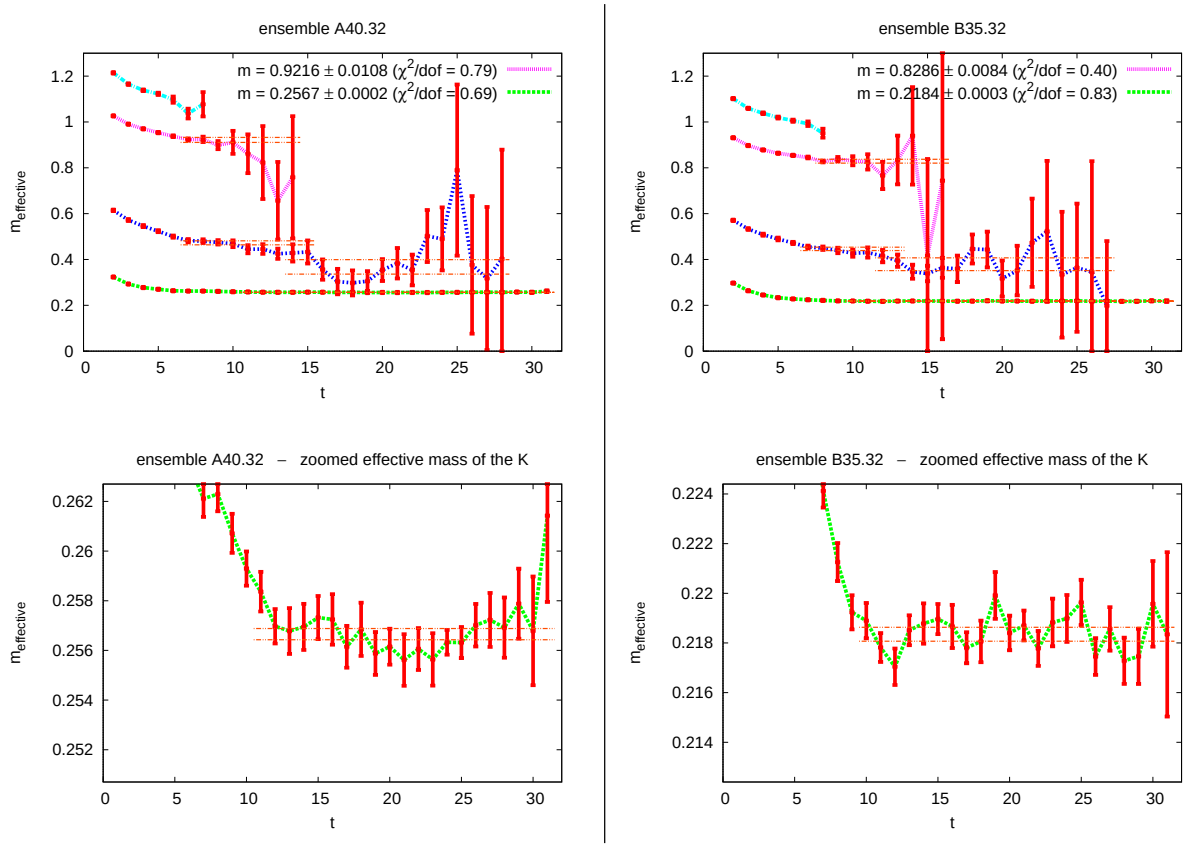

Figure 3: The four effective masses $m^{(n)}_{\text{effective}}$ as functions of t ($t_0 = 1$) for the ensemble A40.32 (left) and B35.32 (right). The zoomed in effective masses for the K meson are also shown in the bottom graphs.

Within this method, a systematic error is associated to the determination of the D meson mass, due to the fact that the effective mass plateau of the $(c, -)$ dominated state will finally decay to lighter strange states at large times, as a consequence of the heavy flavor and parity breaking.

We account for this error by taking the difference with a fit in the range $[t_{\min} - 1, t_{\max}]$, and we combine statistical and systematic uncertainties in quadrature, where the statistical error is obtained by a standard Jackknife analysis.

The results for m_K, m_D and the $(s, +)$ state, which for brevity we denote from now on as K_0^*, are collected in Table 2.

As can also be inferred from Figure 3, we obtain excellent results for m_K. For both ensembles the effective mass plateaus extend over more than twenty points, their statistical errors are essentially independent of t and the relative errors on m_K are $\approx 10^{-3}$. For m_D the situation is more problematic. As shown in Figure 3, the corresponding effective masses are soon lost in statistical noise, before they reach unambiguously identifiable plateaus. As mentioned above, we add for this a systematic uncertainty. The dominantly $(s, +)$ state does not exhibit a true plateau either. One rather observes two different plateaus, and we thus list two results for $m_{K_0^*}$ in Table 2, corresponding to two different fitting ranges. A possible explanation might be that

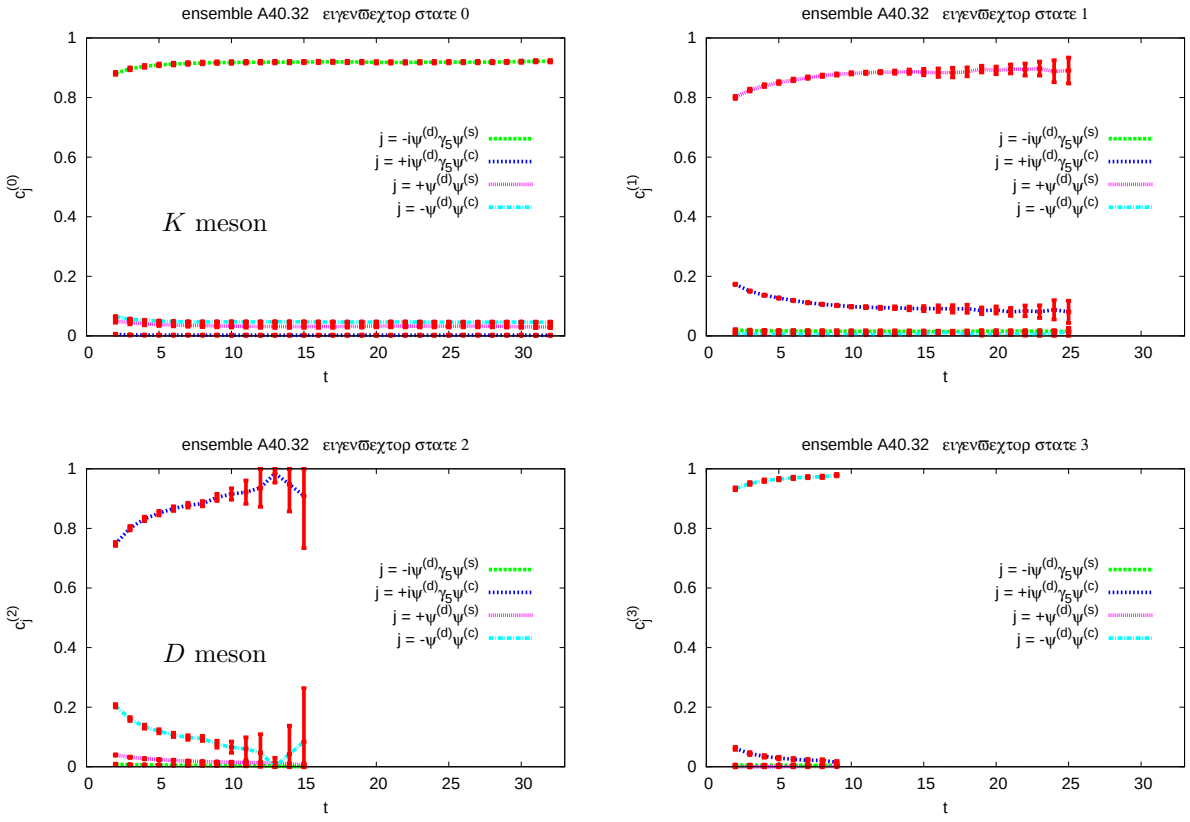

Figure 4: Approximate flavor and parity content of the four extracted states as a function of t ($t_0 = 1$) for the ensemble A40.32. Top left: $n = 0$, mainly $(s, -)$, i.e. the K meson. Top right: $n = 1$, mainly $(s, +)$. Bottom left: $n = 2$, mainly $(c, -)$, i.e. the D meson. Bottom right: $n = 3$, mainly $(c, +)$. The time ranges are the same as for the corresponding effective masses shown in Figure 3.

at small temporal separations $t \lesssim 10$ a positive parity strange meson is seen, while at larger t the lighter $K + \pi$ state, with the same strong quantum numbers, dominates. This is also supported by the fact that at larger values of the light quark mass a single plateau of rather good quality is recovered, see also the results in section 3.3.

3.2 Method 2: fitting the correlation matrix by exponentials

A complementary approach to determine the heavy-light meson masses is to fit the elements of the correlation matrix of eq. (20) by decomposing them in terms of the eigenstates of the Hamiltonian (i.e. the transfer matrix). We consider here the general case with different smearing levels, where $C(t_2 - t_1)$, defined in eq. (20), is a $D \times D$ matrix. When denoting the energy

am_K	t range	χ^2/dof	$am_{K_0^*}$	t range	χ^2/dof	am_D	t range	χ^2/dof
Ensemble A40.32								
0.2567(2)	$11-31$	0.69	0.368(32) 0.473(15)	$14-28$ $7-15$	0.92 1.65	0.922(11)	$7-14$	0.79
Ensemble B35.32								
0.2184(3)	$10-31$	0.83	0.379(28) 0.446(7)	$12-27$ $7-13$	0.54 1.55	0.829(8)	$8-16$	0.40

Table 2: The masses of the K, K_0^* and D mesons in lattice units obtained by solving a generalized eigenvalue problem (errors comprise statistical and systematic errors, which are added in quadrature). The range and the quality of the fit is also shown.

eigenstates by $|n\rangle$, $n = 1, 2, \ldots, M$, the matrix elements of $C(t_2 - t_1)$ can be written as

$$C_{ij}(t_2 - t_1) \;=\; \sum_{n=1}^{M} (i|n)_{t_2}\,(j|n)_{t_1} \tag{33}$$

with

$$(i|n)_t \;\equiv\; \langle\Omega|\mathcal{O}_\chi^{(i)}(t)|n\rangle \;=\; \langle n|\Big(\mathcal{O}_\chi^{(i)}(t)\Big)^\dagger|\Omega\rangle\;, \tag{34}$$

where $i = 1, \ldots, D$ labels the operators inserted in the correlation matrix and $n = 1, \ldots, M$ counts the eigenstates. Since we consider bosonic operators, we have a periodic time dependence on the time extension of the lattice T that can be written as follows

$$(i|n)_{t_2}\,(j|n)_{t_1} \;=\; (i|n)(j|n)\Big(\exp(-(t_2 - t_1)E_n) + \exp(-(T - t_2 + t_1)E_n)\Big)\,. \tag{35}$$

Here, E_n is the energy of the eigenstate $|n\rangle$ and $(i|n) \equiv (i|n)_0$. In general, the number of energy eigenstates is as large as the dimension of the Hilbert space of states. However, for large temporal separations $t_2 - t_1, (T - t_2 + t_1) \gg 1$ a few lowest energy states will dominate to a good approximation. In this limit, and in analogy with the case of fitting a single correlation function with the contributions from a few states, one can fit the matrix of correlation functions with the contributions from the set of dominant lowest energy states. In fact, the relevant number of energy eigenstates M is small. The number N_P of parameters in the fit and the number N_C of independent entries of $C(t_2 - t_1)$ to be fitted are given by

$$N_P \;=\; M(D+1) \quad,\quad N_C \;=\; (t_{\rm max} - t_{\rm min} + 1)\,\frac{D(D+1)}{2}\,, \tag{36}$$

where also here $t_{\rm min}$ and $t_{\rm max}$ define the fitting time interval, with $(t_2 - t_1) \in [t_{\rm min}, t_{\rm max}]$. The minimal set of operators for determining the heavy-light meson masses is given in this case by the 4×4 correlation matrix in terms of the operators in eq. (10). The minimal set of states we are interested in consists of the K and D mesons. At finite lattice spacing, due to the heavy flavor

and parity breaking, the D meson is not stable and does not correspond to an energy eigenstate of the lattice theory. However, using the same arguments of section 3.1, the D should dominate the spectral decomposition of eq. (33) at intermediate temporal separations. In case of fitting the correlation matrix by several exponentials, essential contributions of the lower sectors in the D meson channel can be monitored by considering the scalar products of the linear combination of the operators obtained from the fit with the rows of the maximal twist matrix.

Using the pseudo physical basis operators of eq. (15), one obtains for the coefficients $(i|n)$:

$$(i|n) \equiv \langle\Omega|\mathcal{O}_{\chi}^{(i)}(0)|n\rangle = \sum_{j} \left(\mathcal{M}_{\rm mt}\right)_{ji} \langle\Omega|\mathcal{O}_{\rm ppb}^{(j)}(0)|n\rangle \ . \tag{37}$$

Again, assuming that $\omega_l = \omega_h \approx \pi/2$ and $Z_P/Z_S = 1$ are approximately verified, the operators $\mathcal{O}_{\rm ppb}$ should reproduce the physical operators associated to the four channels $(s,-)$, $(s,+)$, $(c,-)$, $(c,+)$ to a good approximation. In particular, the operator with the same quantum numbers of the state $|n\rangle$ should dominate the sum in (37). We therefore conclude

$$(i|n) \simeq G_n \left(\mathcal{M}_{\rm mt}\right)_{ni} \tag{38}$$

to a good approximation, where the proportionality constant G_n is the matrix element of the physical operator:

$$G_n \equiv \langle\Omega|\mathcal{O}_{\rm ph}^{(n)}(0)|n\rangle \ . \tag{39}$$

It turns out that it is enough to require that the relative signs of the vector components $(i|n)$ agree with the signs in the rows of maximal twist rotation matrix $\mathcal{M}_{\rm mt}$. (A more stringent condition on the alignment with the rows of the maximal twist matrix could be imposed by requiring the scalar products of the linear combinations of the operators obtained from the fit with the rows of the maximal twist matrix to be close to 1, but such a requirement does not essentially change the results for the D meson mass.)

Based on the experience with varying the number of states, we determine the K meson mass with a single intermediate state, while good fits for the D meson mass can be obtained for time separations around $t_2 - t_1 \simeq 10 - 12$, by using three intermediate states. Taking four states gives compatible results, but the signal is lost at smaller distances with consequently larger errors. Larger correlation matrices have also been investigated, for instance, 8×8 matrices spanned by four Gaussian smeared operators of type (10) and the corresponding four local operators. In this case stable fits with one, three or four states can also be obtained.

We minimize the uncorrelated χ^2

$$\chi^2 = \sum_{i=1}^{N_C} \left(\frac{f_i(p_1, p_2, \ldots, p_{N_P}) - \overline{X}_i}{\delta X_i} \right)^2 , \tag{40}$$

where the index i runs over the independent matrix elements to be fitted, $\overline{X}_i$ and δX_i are the mean value and the error of the matrix element i respectively, and $f_i(p_1, p_2, \ldots, p_{N_P})$ is the fitting function depending on N_P parameters defined by eqs. (33) to (35). We determined the

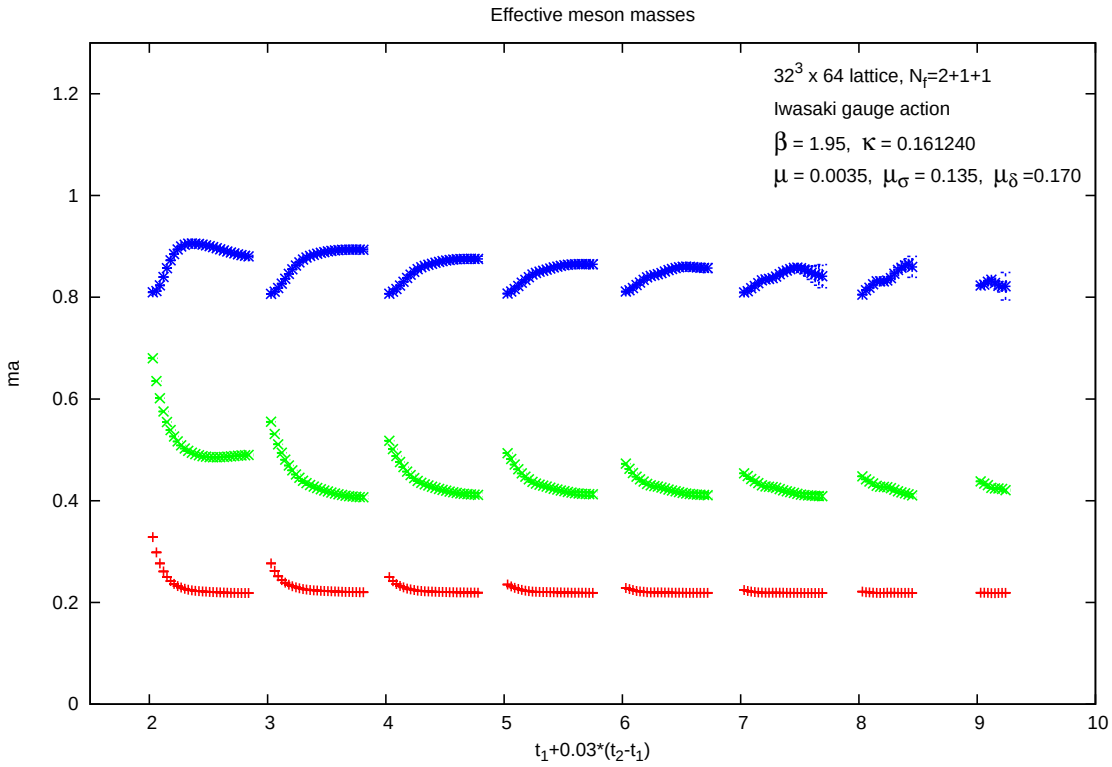

Figure 5: Masses for the K, (bottom), K_0^* (middle) and D (top) channels obtained from a 3×4 fit, i.e. a 4×4 matrix with 3 states, for the ensemble $B35.32$. The fit interval is $[t_1, t_2]$, with values shown by the abscissa. Errors on the masses are also plotted but in most cases are within the symbol size – as show by the figure.

errors of the matrix elements δX_i and of the fit parameters δp_i by the method in ref. [50]. Figure 5 illustrates how the extracted masses depend on the fit intervals. We also studied the correlated χ^2 following refs. [51, 52]

$$\chi_c^2 \;=\; \sum_{i,j=1}^{N_C} \Big(f_i(p) - \overline{X}_i\Big) M_{ij} \Big(f_j(p) - \overline{X}_j\Big), \tag{41}$$

where $M_{ij} = N\mathcal{C}_{ij}^{-1}$, with N input data and the estimated covariance matrix

$$\mathcal{C}_{ij} \;=\; \frac{1}{N-1} \sum_{n=1}^{N} \Big(X_{i,n} - \overline{X}_i\Big)\Big(X_{j,n} - \overline{X}_j\Big). \tag{42}$$

It turned out, however, that on our data samples the covariance matrix has a large number of almost degenerate tiny eigenvalues of the order of magnitude 10^{-16}, which cannot be properly determined within the present statistical accuracy. The small eigenvalues can be smoothed [51, 52], at the price of introducing an uncertainty in the value of χ_c^2. For this reason, we decided

to minimize the uncorrelated χ^2, and to use the correlated one χ^2_c to estimate systematic errors, see below.

Relative errors of the elements of our correlation matrices are typically of $\mathcal{O}(10^{-2})$. This results in rather small errors for the fit parameters on a given time interval: masses have relative errors of $\mathcal{O}(10^{-2})$ to $\mathcal{O}(10^{-3})$, while the components of the energy eigenvectors have errors $\mathcal{O}(10^{-2})$. A good fit has to satisfy for our case the following requirements:

1. The quantum number pattern of the fitting operators has to be as expected, i.e. the relative signs of the components of the fitted vectors are the same as those of the rows of the maximal twist matrix.

2. We exclude the results from fit intervals, where the relative errors of the masses are substantially higher than the typical errors. With our statistics, this means 1% for the K meson mass and 5% for the other masses. Only a few fit intervals turn out to be affected by this choice.

3. The fit ranges $[t_{min}, t_{max}]$ are restricted by applying cuts in t_{min} and $(t_{max} - t_{min})$ such that a reasonable "plateau" of the fit values emerges, always keeping a sufficiently large number of fit ranges in the sample, typically about 30 to 80.

After selecting a set of good fits by these criteria a histogram distribution of the fit values has been defined by attributing a weight $\exp(-\chi^2_c/\mathrm{dof})$ to the entries in case of the kaon, and a weight $1/(\chi^2_c/\mathrm{dof})$ in the other channels. The exponential suppression is in general preferable, since it gives robust results but can only be applied for very good fits and plateaus, which is the case for the kaon. In order to combine statistical and systematic errors, the entries in the distribution were not attributed to a single point but uniformly to the points on the interval $[p_i - \delta p_i, p_i + \delta p_i]$. For each final quantity, the quoted value is then the position of the median of the resulting distribution. The error is given by a symmetric interval around the median such that 68% of the distribution is contained in it.

We report on single-state, three-state, and four-state fits with a 4×4 correlation matrix of Gaussian smeared operators. For completeness, we also show the results of three-state fits with an 8×8 matrix of Gaussian smeared and local operators. All results are summarized in Table 3.

As shown in table 3 the four-state fit to a 4×4 matrix gives one state in each of the channels $J^{\mathcal{P}} = 0^-$ and $J^{\mathcal{P}} = 0^+$, with both strange and charmed quarks. On the other hand, errors are typically larger and/or the light states have higher masses than in the 1×4 and 3×4 fits. Therefore, as final results we quote the K meson mass from the 1×4 fit and the D meson mass from the 3×4 fit.

One can verify a posteriori how well the quantum number content of each fitted vector corresponds to the expected one. This is simply given by the scalar product of the unit vector in the direction of the fitted vector with the row of the matrix in eq. (15) that gives the expected vector in the continuum limit at maximal twist. For this, we remind that the K meson, strange 0^+ state, D meson and charmed 0^+ state correspond to the rows 1, 3, 2 and 4, respectively. Table 4 shows that the fitted vectors are actually well saturated by the expected quantum numbers, with scalar products close to 1 in all cases.

Ensemble	$M \times D$	am_K	$am_{K_0^*}$	am_D	$am_{D_0^*}$
A40.32	1x4	0.25542(67)			
	3x4	0.25853(88)	0.448(13)	0.903(20)	
	4x4	0.26272(62)	0.4905(60)	0.939(46)	1.09(15)
	3x8	0.2627(23)	0.478(18)	0.885(22)	
B35.32	1x4	0.21766(64)			
	3x4	0.21864(51)	0.422(11)	0.835(20)	
	4x4	0.2226(69)	0.449(24)	0.896(70)	1.19(10)
	3x8	0.2203(13)	0.4369(94)	0.814(18)	

Table 3: Masses of the K, K_0^*, D and D_0^* in lattice units, resulting from the fits to the correlation matrices with several eigenstates for the ensembles A40.32 and B35.32. The label $M \times D$ means a fit with M eigenstates to a $D \times D$ matrix.

Ensemble	$M \times D$	z_K	$z_{K_0^*}$	z_D	$z_{D_0^*}$
A40.32	1x4	0.98659(6)			
	3x4	0.9871(2)	0.9896(17)	0.9392(78)	
	4x4	0.9870(2)	0.9845(23)	0.9929(1)	0.9830(133)
B35.32	1x4	0.98518(8)			
	3x4	0.9847(1)	0.9772(33)	0.9518(94)	
	4x4	0.9848(1)	0.9770(21)	0.9777(86)	0.9732(110)

Table 4: Saturation of the fitted states with the expected quantum numbers, for the four-states fits of table 3, measured by the scalar product z (see text). A value $z = 1$ indicates complete saturation. Mean values and errors for z are determined analogously to masses.

3.3 Method 3: parity and flavor symmetry restoration

This third method is a generalization of the "parity restoration method" originally introduced for the twisted mass formulation with two degenerate quarks [53, 54, 55]. In the $N_{\rm f} = 2$ setup the twist angle can be determined by requiring that the operators reproducing the correct definition of the chiral currents in the continuum limit (physical chiral currents) possess the appropriate transformation properties under parity. This condition allows to fix the twist angle for the degenerate light quark doublet and the correctly normalized physical currents. We generalize the method to the case of bilinear densities with mixed heavy-light flavor composition, used here for the determination of the K and D meson masses. A first account of this method can be found in [35]. As an outcome, approximations of the physical operators in eq. (9) can be constructed, from which the masses in the four heavy-flavor and parity channels can be extracted by conventional techniques.

Consider the four-by-four correlation matrix of the renormalized lattice operators in eq. (14):

$$C^R(t_2 - t_1) \;=\; \left\langle \mathcal{O}^R(t_2) \otimes (\mathcal{O}^R(t_1))^\dagger \right\rangle . \tag{43}$$

After rewriting the renormalized lattice operators in terms of the bare ones one obtains

$$C^R(t_2-t_1) \;=\; \mathrm{diag}\Big(Z_P,Z_P,Z_S,Z_S\Big)\,C(t_2-t_1)\,\mathrm{diag}\Big(Z_P,Z_P,Z_S,Z_S\Big)\;, \tag{44}$$

where $C(t_2-t_1)$ is the correlation matrix defined in eq. (20), the starting point of the previous two methods. The transformation properties of the correlation matrix (43) can be read from eq. (13), implying that the correlation matrix of the physical operators (9) is given by

$$\begin{aligned} C^R_{\rm ph} \;&=\; \mathcal{M}(\omega_l,\omega_h)\,C^R\,\mathcal{M}^T(\omega_l,\omega_h) \;= \\ &\mathcal{M}(\omega_l,\omega_h)\,\mathrm{diag}\Big(Z_P,Z_P,Z_S,Z_S\Big)\,C\,\mathrm{diag}\Big(Z_P,Z_P,Z_S,Z_S\Big)\mathcal{M}^T(\omega_l,\omega_h)\;, \end{aligned} \tag{45}$$

where, we recall, the general orthogonal twist rotation matrix $\mathcal{M}(\omega_l,\omega_h)$ is given by (12). Since we are working at maximal twist, we are supposed to insert $\omega_l=\omega_h=\pi/2$ in the rotation matrix of eq. (45). However, differently from the previous two methods and accounting for the presence of $\mathcal{O}(a)$ effects, we treat the two twist angles, along with the renormalization factors Z_P and Z_S, as free parameters. We will return to this point in the following. These free parameters can be determined by imposing that the physical operators indeed possess the appropriate parity and flavor quantum numbers of their associated channel. This in particular implies that the physical correlation matrix of eq. (45) should be diagonal

$$\Big(C^R_{\rm ph}\Big)_{jk} \;=\; 0\;,\quad j\neq k\;. \tag{46}$$

Since $C(t_2-t_1)$ is a symmetric matrix (see section 2.2.1), the matrix in eq. (45) is by construction symmetric and eq. (46) actually amounts to only six independent conditions. The latter can be rearranged as follows

$$\frac{Z_P^2}{Z_S^2} \;=\; -\frac{C_{34}}{C_{12}} \tag{47}$$

$$\mathrm{ctg}(\omega_l) \;=\; +\frac{(+C_{11}-C_{22})(Z_P/Z_S)+(-C_{33}+C_{44})(Z_S/Z_P)}{2(C_{13}-C_{24})} \tag{48}$$

$$\mathrm{ctg}(\omega_h) \;=\; +\frac{(+C_{11}-C_{22})(Z_P/Z_S)+(+C_{33}-C_{44})(Z_S/Z_P)}{2(C_{14}-C_{23})} \tag{49}$$

$$\begin{aligned} &\tan(\omega_l+\omega_h) \;= \\ &\quad= \;-\frac{C_{14}+C_{23}+C_{13}+C_{24}}{(+C_{11}+C_{22})(Z_P/Z_S)+(-C_{33}-C_{44})(Z_S/Z_P))/2+C_{12}(Z_P/Z_S)-C_{34}(Z_S/Z_P)} \end{aligned} \tag{50}$$

$$\begin{aligned} &\tan(\omega_l-\omega_h) \;= \\ &\quad= \;+\frac{C_{14}+C_{23}-C_{13}-C_{24}}{(+C_{11}+C_{22})(Z_P/Z_S)+(-C_{33}-C_{44})(Z_S/Z_P))/2-C_{12}(Z_P/Z_S)+C_{34}(Z_S/Z_P)} \end{aligned} \tag{51}$$

$$\frac{\tan(\omega_l)}{\tan(\omega_h)} \;=\; -\frac{C_{13}+C_{24}}{C_{14}+C_{23}}. \tag{52}$$

Observe that the right hand sides of (48) to (52) are fully determined by the ratio Z_P/Z_S, i.e. they do not depend individually on either Z_P or Z_S.

In Figure 6 we report on the ratios of correlators on the right hand sides of the conditions (47) to (52) as functions of the time separation $t \equiv t_2 - t_1$, for the ensemble A40.32 and the original operators without Gaussian smearing. The ratios appear to approach a plateau after a transient: from these plateaus we determine the unknown parameters Z_P/Z_S, ω_l and ω_h.

Notice that the time dependence of the ratios is an $\mathcal{O}(a)$ discretization effect, and therefore not predicted by eqs. (47)-(52), which were derived in the continuum limit. For large times the lightest eigenstate of the lattice transfer matrix, corresponding to the kaon in the continuum, is supposed to saturate the spectral decomposition of the correlation matrix $C(t_2 - t_1)$ (see eqs. (33) and (34)). Assuming a single intermediate state, the six conditions (47)-(52) are not independent any more and in particular the first three of relations (47)-(49) are equivalent to (50)-(52). Parity and flavor restoration amounts in this case to requiring that the three physical operators associated to the heavier channels have no projection on the lightest state, namely

$$\sum_{\mathbf{x}} \langle \Omega | \mathcal{O}_{\rm ph}^{(s,1)}(\mathbf{x},t) | K \rangle \;=\; \sum_{\mathbf{x}} \langle \Omega | \mathcal{O}_{\rm ph}^{(c,\gamma_5)}(\mathbf{x},t) | K \rangle \;=\; \sum_{\mathbf{x}} \langle \Omega | \mathcal{O}_{\rm ph}^{(c,1)}(\mathbf{x},t) | K \rangle \;=\; 0 \;. \qquad (53)$$

We also observe that this procedure, which relies on asymptotic times, is supposed to be optimal from the point of view of the cutoff effects: at large times, contribution from high-mass intermediate states, which are expected to introduce large discretization effects in the correlator, is suppressed. A similar argument was used when tuning the theory to maximal twist in the light sector, see [2].

We determine Z_P/Z_S, ω_l and ω_h by using the relations (47-49), while the remaining relations serve for cross checking of the results. The latter are reported in Table 5. We observe an excellent agreement between the different determinations of the twist angles from (48-49) and (50-51), respectively, confirming that a single intermediate state contributes. The quality of the agreement deteriorates, of course, when the parameters are estimated at smaller temporal separations outside the asymptotic region. Notice that the ratio $\tan(\omega_l)/\tan(\omega_h)$ is in all cases compatible with zero, since $\omega_h \approx \pi/2$. Note instead that the value of the light twist angle

eqs.	Z_P/Z_S	eqs.	ω_l/π	ω_h/π	$\tan(\omega_l)/\tan(\omega_h)$
ensemble A40.32					
(47)	0.6575(14)	(48-49)	0.6504(21)	0.4980(8)	-0.012(5)
(47)	same value	(50-51)	0.6498(22)	0.4990(10)	-0.006(5)
(47)	same value	(52)	–	–	-0.009(5)
ensemble B35.32					
(47)	0.6793(22)	(48-49)	0.6453(34)	0.5005(8)	0.003(5)
(47)	same value	(50-51)	0.6467(29)	0.5007(9)	0.005(6)
(47)	same value	(52)	–	–	0.005(5)

Table 5: summary of different determinations of the ratio of renormalization factors and of the twist angles with point-like operators (no Gaussian smearing); the first and third column indicate the equations used for the determination of the quantities in the corresponding line.

in Table 5 significantly deviates from the expected value $\pi/2$. In order to understand this discrepancy it is useful to recall that the theory is tuned to maximal twist by requiring the vanishing of the untwisted PCAC quark mass $m_{\chi^{(l)}}^{PCAC}$ *in the light quark sector*, see eq. (4)).

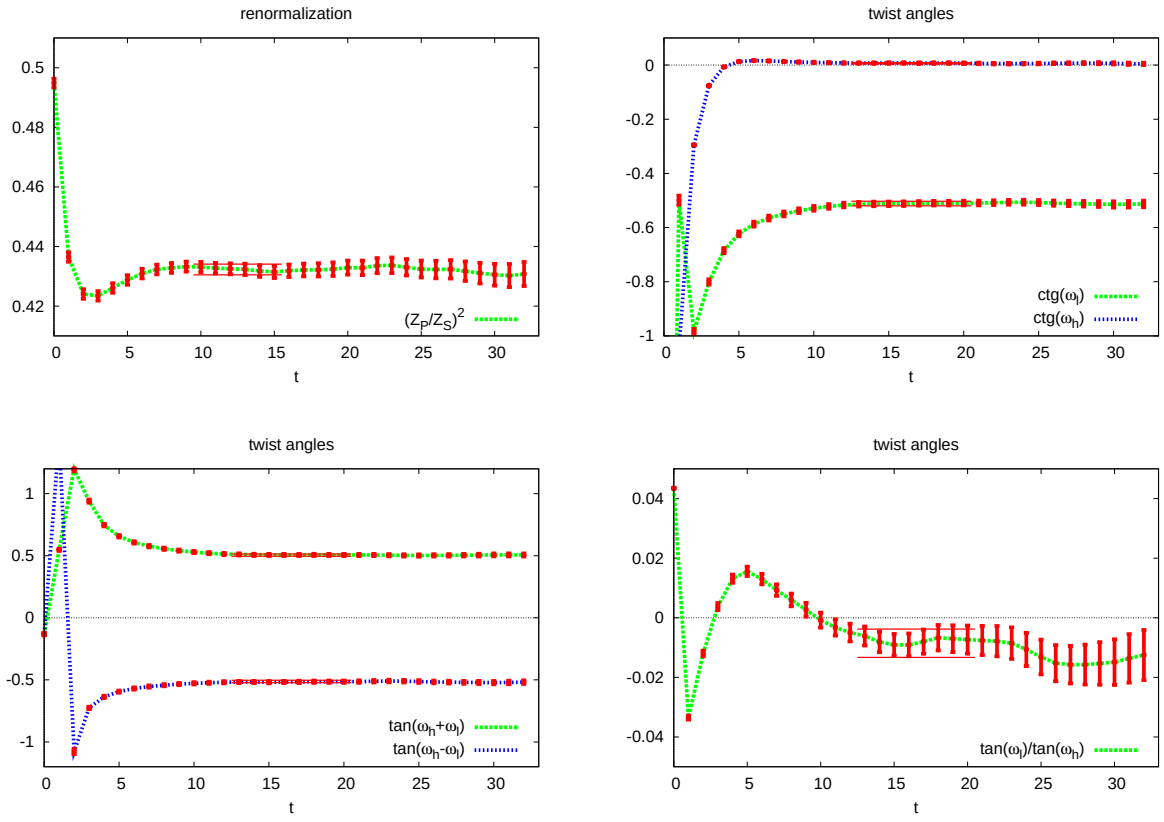

Figure 6: ratios of correlators corresponding to the right hand sides of the conditions (47) to (52) as functions of the temporal separation t for ensemble A40.32 with point-like operators (i.e. no Gaussian smearing); the lines indicate the fits in the asymptotic regime.

This can be shown to be equivalent [55] to requiring parity restoration in the light quark sector. One constructs in this case the physical vector current as follows [55]

$$V_{ph}^{(l)+}(x) \;\propto\; \cos(\omega_l)\, Z_V\, V^{(l)+}(x) \;- i\, \sin(\omega_l)\, Z_A\, A^{(l)+}(x)\;, \tag{54}$$

where the bilinear of the lattice fields $A^{(l)+}(x)$ is defined in eq. (5) and, analogously,

$$V_\mu^{(l)+} \;=\; \bar{\chi}^{(u)}\gamma_\mu\chi^{(d)}\;, \tag{55}$$

and Z_A, Z_V are the respective renormalization constants in the massless scheme. The twist angle ω_l is fixed in this case by the condition

$$\sum_{\mathbf{x}}\langle\Omega|V_0^{(l)+}(\mathbf{x},t)|\pi\rangle \;=\; 0\;, \tag{56}$$

from which one obtains

$$\mathrm{ctg}(\omega_l) \;=\; \frac{Z_A\, m_{\chi^{(l)}}^{\mathrm{PCAC}}}{\mu}\;. \tag{57}$$

From this we can conclude that our maximal twist condition $m_{\chi^{(l)}}^{\rm PCAC}=0$ amounts to $\omega_l=\pi/2$, if the condition (56) is assumed. This must be confronted with the conditions (53) presently used to fix the twist angles ω_l[2]. We conclude that the deviation of ω_l from $\pi/2$ should be attributed to different $\mathcal{O}(a)$ effects in the pion and kaon sectors.

We stress that the prescription of eq. (4), which is based on the charged pion state, is to be preferred for tuning the theory to maximal twist, since it ensures the smallest $\mathcal{O}(a^2)$ discretization errors in physical quantities [32]. Nevertheless, for the determination of the masses in the heavy-light meson sector, we use the values of the twist angles obtained from (47) to (52), since they deliver optimal projecting operators as defined in eq. (13), with the smallest heavy flavor and parity violations. The relation in (57) can also be enforced for the present determination of the light twist angle with heavy-light quark bilinears, and the cutoff effects can be absorbed in a lattice redefinition of the PCAC quark mass, $\tilde{m}_{\chi^{(l)}}^{\rm PCAC}=m_{\chi^{(l)}}^{\rm PCAC}+\mathcal{O}(a)$. For the ensemble A40.32, we get for instance $Z_A\tilde{m}_{\chi^{(l)}}^{\rm PCAC}/\mu\approx -0.5$, a pretty large value[3]. The analogous of relation (57) for the heavy twist angle reads

$$\mathrm{ctg}(\omega_h) \;=\; \frac{Z_A\tilde{m}_{\chi^{(l)}}^{\rm PCAC}}{\mu_\sigma}\,. \tag{58}$$

The heavy twisted mass μ_σ replaces the light twisted mass μ, explaining why ω_h is very close to $\pi/2$: since $\mu_\sigma\gg\mu$, the non-zero value of $\tilde{m}_{\chi^{(l)}}^{\rm PCAC}$ only results in a small deviation of ω_h from maximal twist. When inserting the above estimate in (58) we indeed obtain $\omega_h=0.4956$.

The ratio of normalization factors Z_P/Z_S and the twist angles ω_l and ω_h allow to determine the physical operators up to an overall renormalization (bare physical operators). We choose this renormalization to be Z_P, so that (cf. eqs. (13) and (14))

$$\mathcal{O}_{\rm ph}^{bare} \;\equiv\; Z_P^{-1}\,\mathcal{O}_{\rm ph}^{R} \;=\; \mathcal{M}(\omega_l,\omega_h)\,\mathrm{diag}\Big(Z_P/Z_S, Z_P/Z_S, 1, 1\Big)\,\mathcal{O}_\chi\;. \tag{59}$$

Observe that in the case of the negative parity densities, eq. (59) corresponds to the conventional relation between renormalized and bare operators

$$\mathcal{O}_{\rm ph}^{(h,\gamma_5)\,bare} \;=\; Z_P^{-1}\,\mathcal{O}_{\rm ph}^{(h,\gamma_5)\,R}\;; \tag{60}$$

on the other hand, the conventional definition for the bare scalar densities, for which

$$\mathcal{O}_{\rm ph}^{(h,1)\,bare,\,conv.} \;=\; Z_S^{-1}\,\mathcal{O}_{\rm ph}^{(h,1)\,R} \tag{61}$$

holds, is related to the definition (59) by a finite renormalization

$$\mathcal{O}_{\rm ph}^{(h,1)\,bare,\,conv.} \;=\; Z_P/Z_S\,\mathcal{O}_{\rm ph}^{(h,1)\,bare}\;. \tag{62}$$

[2]In the asymptotic regime, where only the kaon state is considered as intermediate state, the light twist angle ω_l is fixed by the vanishing of the first two matrix elements in (53); this is so because, in this regime, the two conditions can be proven to imply in particular relations (47) and (48) (analogously, ω_h is fixed in particular by the vanishing of the second and third matrix element).

[3]For comparison, in the tuning procedure we require $Z_A|m_{\chi^{(l)}}^{\rm PCAC}|/\mu\leq 0.1$.

Of course, with Z_P/Z_S at hand both definitions can be computed.

Figure 7 shows the diagonal and off-diagonal correlators of the bare physical operators for the ensemble B35.32 with Gaussian smearing, which are the ones used for the final computation of all masses. A general feature is that starting from time separation $t \gtrsim 5$ most of the off-diagonal elements become small and compatible with zero within statistical errors. An exception is the matrix element $\langle \mathcal{O}_{\rm ph}^{(c,\gamma_5)} (\mathcal{O}_{\rm ph}^{(s,1)})^\dagger \rangle$, which remains large and comparable in size with the two smallest diagonal elements in the $(c, -/+)$ sectors. At the moment we have no explanation for this observation.

It should also be noted that, following the arguments of [47, 46], $\mathcal{O}(a)$ improvement can only be expected for the diagonal elements of the physical correlation matrix. Since the twist angles and the ratio Z_P/Z_S are obtained from conditions on the off-diagonal elements, one should a priori expect $\mathcal{O}(a)$ discretization errors for these quantities. However, it should be stressed that for physical quantities such as meson masses and decay constants, which are extracted from the diagonal matrix elements, $\mathcal{O}(a)$ improvement is at work. The mass of the low-lying state in each

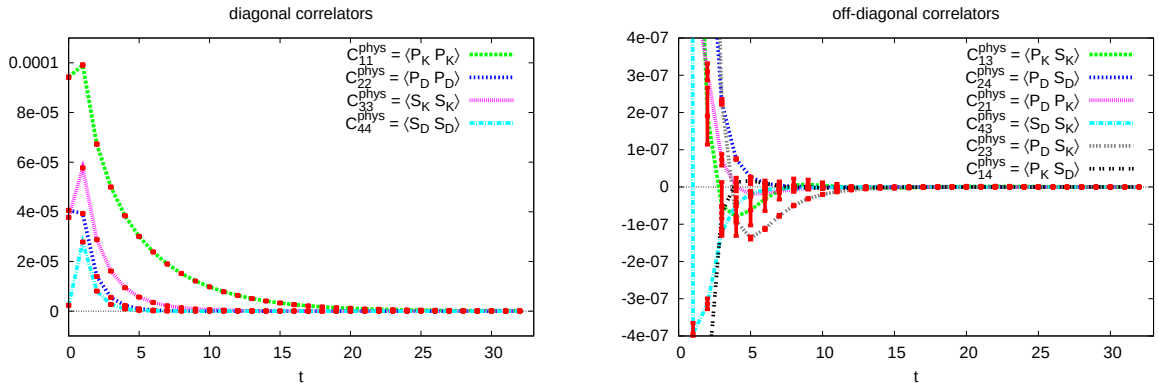

Figure 7: Bare physical correlators for the ensemble B35.32 with Gaussian smeared operators.

of the four different channels can now be extracted by standard techniques from the diagonal correlator of the appropriate operator in (59). The effective masses for the four channels and the two ensembles are reported in Figure 8, for negative parity, and Figure 9, for positive parity. The final values for all masses are obtained by applying single-mass fits with a cosh function in the asymptotic regime. Also in this case the statistical error of the fitting parameters is determined by the linearization method of [50]. The starting time t_{min} for the fits was chosen by requiring $\chi^2/\mathrm{dof} \lesssim 1$.

The plateaus for the charmed meson states are generally quite short, since the noise sets in early, typically around $t \gtrsim 11$. This is, however, expected. For those temporal separations the D correlator is only a small fraction of the kaon correlator, as shown in the left panel of Figure 7. On the other hand, the D correlator results from a linear combination of the correlators of the twisted basis χ-field bilinears in eq. (10), all dominated by the kaon. This means that the condition (53) can only be fulfilled through a cancellation of large terms, one of the results being the comparably small D correlator. The latter inherits the statistical fluctuations of the original bilinears and a large relative error is the consequence. As already stated many times in this

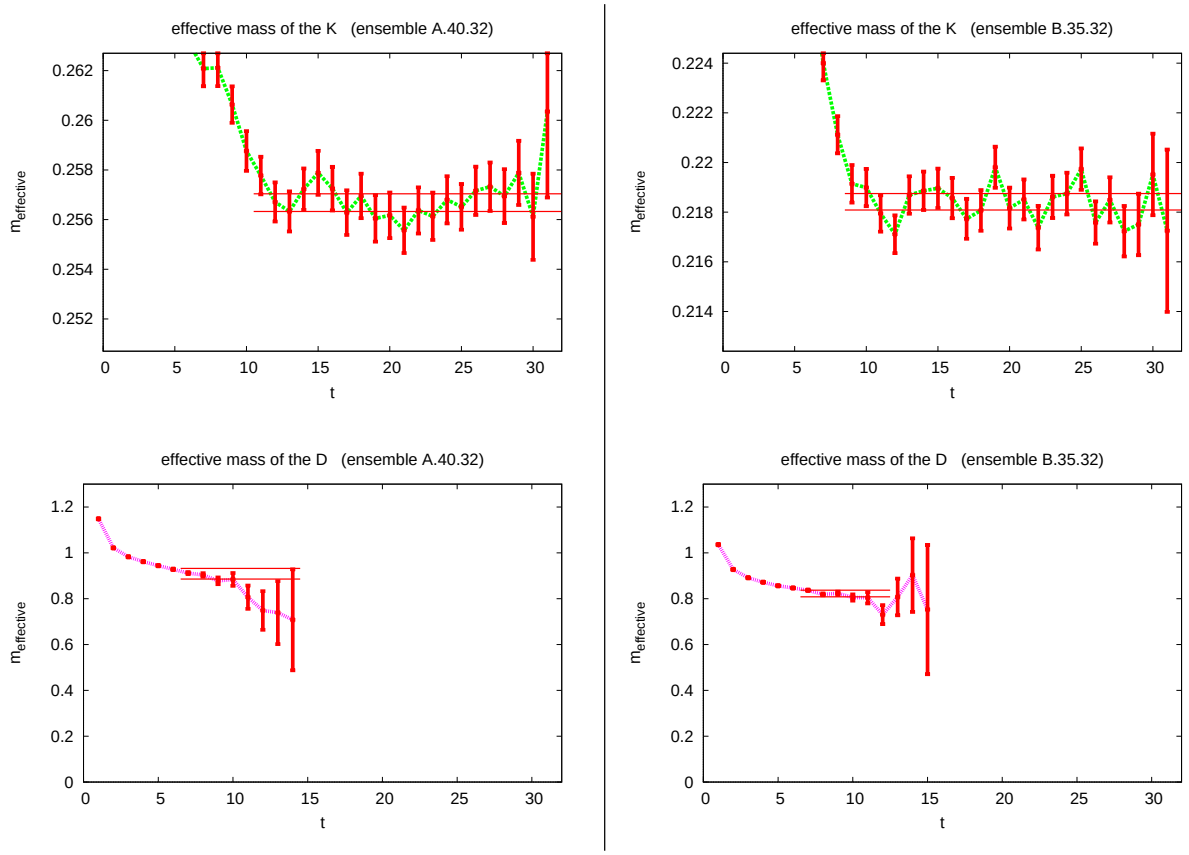

Figure 8: The effective masses in the pseudoscalar channel, with Gaussian smeared operators, for the ensembles A40.32 (left) and B35.32 (right). The error bands indicate the total error, statistical plus systematic.

paper, this is an inherent problem in our twisted mass setup, where the D is actually a highly excited state in the mixed $(s/c, -/+)$ heavy-light meson sector.

In the case of the D meson we attempt to estimate the systematic error produced by possible residual contributions of excited states and the influence of an unphysical mixing with the rather light K_0^* state[4]. We apply a procedure analogous to the one of section 3.2, and consider the spread of results by including all good fits (those with high significance) obtained by varying the fit interval $[t_{\rm min}, t_{\rm max}]$. The resulting systematic error is much larger than the statistical one, and decreases on the finer lattice. This is reflected by the better quality of plateaus for the ensemble B35.32, as compared to A40.32, see Figure 8.

The numerical results for all masses are listed in Table 6. For K_0^* different plateaus could be identified for the effective mass. In this case the value for each plateau is reported. It is unclear at this stage, whether this multi plateau behavior reflects the physical structure of QCD states in this sector, or is just a statistical effect, as also discussed at the end of section 3.1.

We conclude the illustration of this method by briefly discussing its generalization to the case of

[4]The mixing with the kaon has been eliminated by construction.

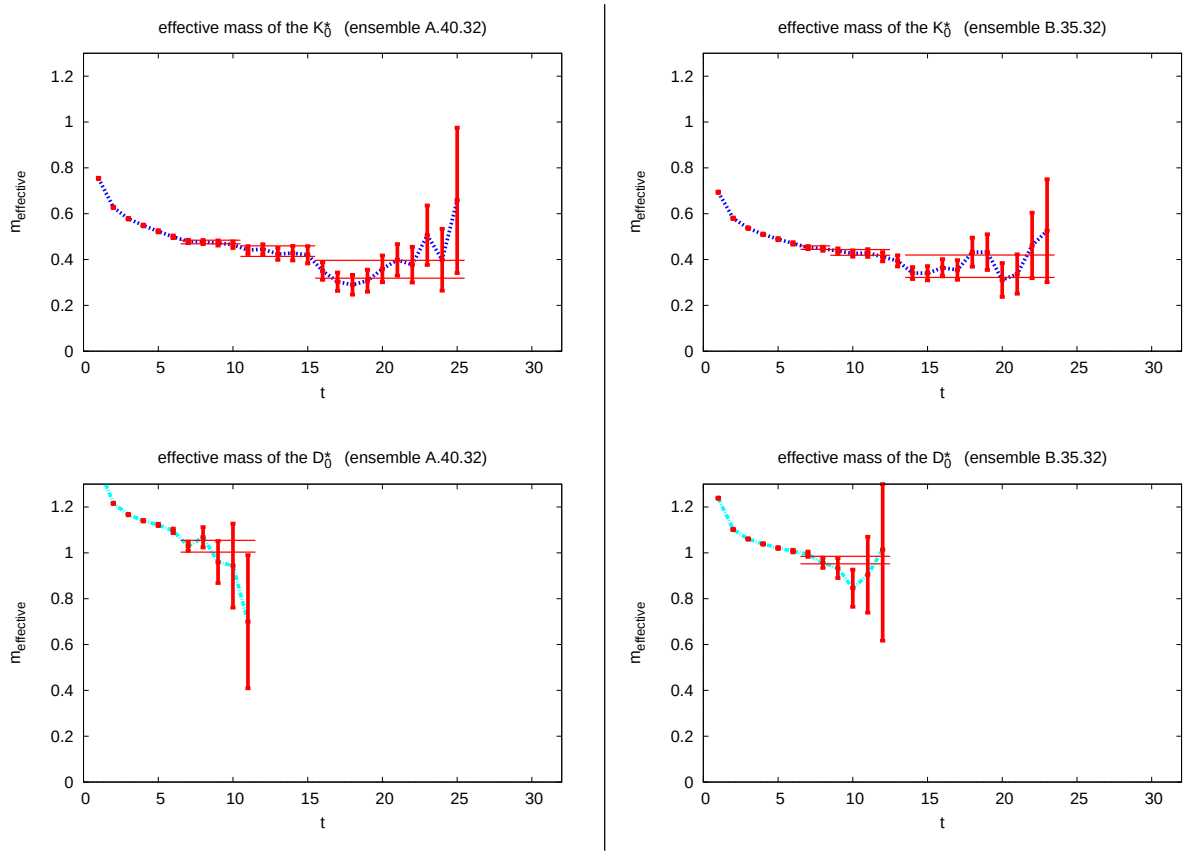

Figure 9: The effective masses in the scalar channel, with Gaussian smeared operators, for the ensembles A40.32 (left) and B35.32 (right). The error bands indicate the total error, statistical plus systematic.

$4 \times n$ operators, the immediate application being the one considered in the previous section with both local and smeared operators. The obvious route would just be to diagonalize each 4×4 correlation sub-matrix with homogeneous composition (e.g. local or smeared operators only) as we have done so far. As a result, the twist angles and the Z_P/Z_S factors are obtained for each set; observe that the Z_P/Z_S factors are heavily affected by the smearing, which brings the former closer to one. Also the twist angles are expected to differ, due to different $\mathcal{O}(a)$ effects for local and smeared operators. Once these parameters are known, the physical correlation matrices with mixed local/smeared operators can be reconstructed, too. However, this procedure is not expected to be optimal for the latter correlation matrices, since the parameters are adjusted to optimize the correlation matrices with homogeneous composition. A better way would be to apply an independent diagonalization, with new parameters, of the matrices with mixed local/smeared composition.

Ensemble	am_K	t_1, t_2	$am_{K_0^*}$	am_D	$am_{D_0^*}$
A40.32	0.25668(35)	7-8	0.452(8)	0.909(4)(22)	1.029(26)
		9-12	0.431(12)		
		14-32	0.37(5)		
B35.32	0.21842(33)	7-10	0.476(8)	0.823(4)(14)	0.968(16)
		11-15	0.437(23)		
		16-32	0.358(39)		

Table 6: Masses of the K, K_0^*, D and D_0^* mesons in lattice units, obtained with the parity and flavor restoration method, and using Gaussian smeared operators. The third row contains the temporal separations used for the determination of $m_{K_0^*}$.

4 Conclusions

We have proposed and compared three methods to determine m_K and m_D in $N_\mathrm{f} = 2 + 1 + 1$ twisted mass lattice QCD. The computation of these masses is less straightforward in this case, since parity and flavor are not good quantum numbers. We have therefore explored strategies to extract the desired states and have developed three distinct methods all of which exploit the exponential fall-off of correlation matrices for suitably chosen heavy-light meson creation operators. Method 1 amounts to solving a generalized eigenvalue problem, method 2 is equivalent to fitting a linear superposition of exponentials and method 3 transforms the correlators to the physical basis by means of the twist rotation. Results for m_K and m_D obtained with the three methods and for both ensembles investigated here are summarized in Table 7 and visualized in Figure 10. Since the kaon is the lightest state in the combined $(s/c, -/+)$ sector, the

	Method 1	Method 2	Method 3
Ensemble A40.32			
am_K	0.2567(2)	0.25554(88)	0.25668(35)
am_D	0.922(11)	0.901(21)	0.909(22)
Ensemble B35.32			
am_K	0.2184(3)	0.21768(84)	0.21842(33)
am_D	0.829(8)	0.835(20)	0.823(15)

Table 7: Comparison of the results for m_K and m_D obtained with the three methods exposed in this work, for both ensembles.

computation of its mass is rather simple and we obtain precise values for m_K with errors $\lesssim 0.4\%$ including statistical and systematical uncertainties. Moreover, within these errors all three methods yield very compatible results which is very reassuring.

In contrast to m_K, the mass of the D meson is difficult to determine, because in our twisted mass setup the D meson is a highly excited state in the combined $(s/c, -/+)$ sector. However, also in this case our three methods yield results, which are in excellent agreement within the combined statistical and systematical errors, whose relative magnitudes are $\lesssim 2.5\%$. Therefore, we are

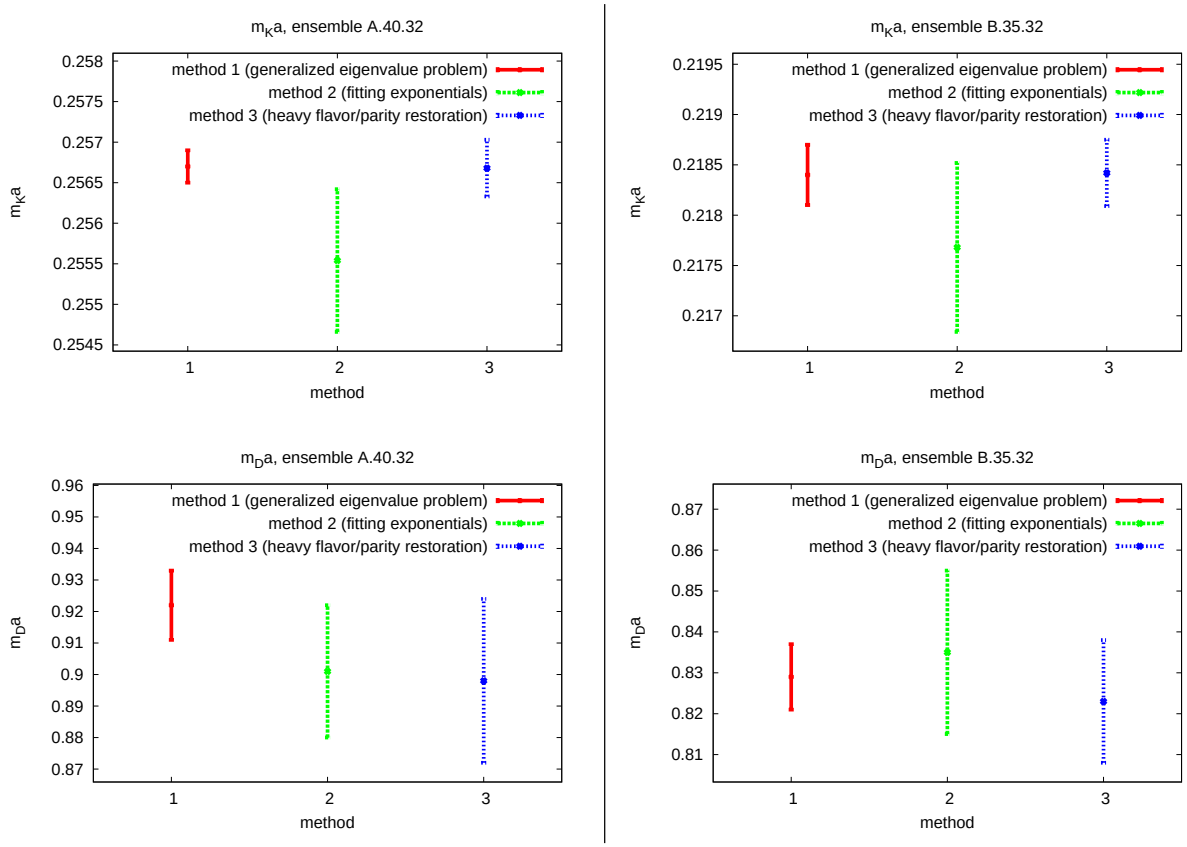

Figure 10: Comparison of the results for m_K (top) and m_D (bottom) obtained with the three methods exposed in this work, for both ensembles. The results for methods 1 to 3 are shown from left to right.

confident that we are able to obtain reliable estimates for m_D without resolving all the low lying (multi particle) states below the D meson. The latter would require to compute correlation matrices with a significantly larger operator basis and with extremely high statistical precision, an endeavor, which hardly seems to be feasible. It is therefore very important that already with the much smaller correlator matrix employed here, one can obtain a satisfactory estimate of the D meson mass.

The errors we obtain with our three methods differ by factors of around 2 to 4, originating from the fact that the three methods estimate the systematic error in different ways. While method 2 (fitting exponentials) tends to yield the largest error, its procedure to determine the systematic error is also the most conservative: the error is computed from the spread of a large set of fit results corresponding to different fitting ranges. In contrast to that method 1 (solving a generalized eigenvalue problem) estimates the corresponding error by just taking two "neighboring fitting ranges" into account. Consequently, the total error is somewhat smaller.

We stress that as far as K physics is concerned, our analysis shows that this sector can be analyzed in the unitary setup without problems. This provides a very good perspective to compute corresponding decay constants and also the strange baryon spectrum in the future. For

charm physics, the situation is different and it will be quite difficult to extract reliable physics results in the charm sector from the unitary setup. Here, we plan to employ a mixed action approach by using an Osterwalder-Seiler (OS) valence quark action [34]. This has the advantage [56] that there is no flavor mixing and that the valence quarks stay as close as possible to the sea twisted mass quarks, e.g. there is no need to re-tune κ to realize maximal twist. The idea is to match the K and D meson masses between the unitary setup and the valence OS quarks. After this matching step further physical quantities such as decay constants will then be computed with OS quarks. The matching condition will guarantee that in the continuum limit we recover the situation of a unitary setup. Of course, it needs to be seen, whether discretization errors in this strategy remain small. Investigations in this direction are in progress.

With respect to the matching of K and D meson masses between the unitary setup and the valence OS quarks, the outcome of our work in this paper is extremely important. The fact that we can compute the K meson with high accuracy and the D meson with acceptable precision in the unitary setup is a necessary prerequisite to allow for applying such a matching condition.

Instead of matching the K and D meson masses in the sea and valence sectors, one can directly match the renormalized strange and charm quark masses [34]. The latter can be determined in the sea sector by using eq. (6). Only the finite ratio Z_P/Z_S is needed as an input for the matching. We have shown in this paper one possible way to determine this quantity, which is specific for the twisted mass setup. In compliance with the massless quark renormalization scheme, however, the extrapolated value of Z_P/Z_S for four massless quarks is required. We mention here that the ETMC has started a dedicated program to evaluate the renormalization constants for our $N_{\rm f} = 2 + 1 + 1$ setup in the massless quark limit. Once the relevant renormalization constants will be available, this information will be used for an alternative tuning of the mass parameters in the valence sector. This can result in different values of the valence quark masses with respect to the procedure relying on the hadron masses, and hence to different cut-off effects for the resulting mixed action theory. Employing both matching conditions can therefore be used to have independent computations for physical observables and will provide a most valuable cross-check of the way this setup approaches the continuum limit.

Acknowledgments

The computer time for this project was made available to us by the John von Neumann-Institute for Computing (NIC) on the JUMP, Juropa and Jugene systems in Jülich and apeNEXT system in Zeuthen, BG/P and BG/L in Groningen, by BSC on Mare-Nostrum in Barcelona (www.bsc.es), and by the computer resources made available by CNRS on the BlueGene system at GENCI-IDRIS Grant 2009-052271 and CCIN2P3 in Lyon. We thank these computer centers and their staff for all technical advice and help.

This work has been supported in part by the DFG Sonderforschungsbereich/ Transregio SFB/TR9-03 and the EU Integrated Infrastructure Initiative Hadron Physics (I3HP) under contract RII3-CT-2004-506078. We also thank the DEISA Consortium (co-funded by the EU, FP6 project 508830), for support within the DEISA Extreme Computing Initiative (www.deisa.org).

References

[1] **ETM** Collaboration, Ph. Boucaud *et al.*, "Dynamical twisted mass fermions with light quarks," Phys. Lett. B **650**, 304 (2007) [arXiv:hep-lat/0701012].

[2] **ETM** Collaboration, Ph. Boucaud *et al.*, "Dynamical twisted mass fermions with light quarks: simulation and analysis details," Comput. Phys. Commun. **179**, 695 (2008) [arXiv:0803.0224 [hep-lat]].

[3] **ETM** Collaboration, R. Baron *et al.*, "Light meson physics from maximally twisted mass lattice QCD," arXiv:0911.5061 [hep-lat].

[4] **ETM** Collaboration, C. Alexandrou *et al.*, "Light baryon masses with dynamical twisted mass fermions," Phys. Rev. D **78**, 014509 (2008) [arXiv:0803.3190 [hep-lat]].

[5] **ETM** Collaboration, C. Alexandrou *et al.*, "The low-lying baryon spectrum with two dynamical twisted mass fermions," Phys. Rev. D **80**, 114503 (2009) [arXiv:0910.2419 [hep-lat]].

[6] **ETM** Collaboration, B. Blossier *et al.*, "Light quark masses and pseudoscalar decay constants from $N_{\rm f} = 2$ lattice QCD with twisted mass fermions," JHEP **0804**, 020 (2008) [arXiv:0709.4574 [hep-lat]].

[7] **ETM** Collaboration, B. Blossier *et al.*, "Pseudoscalar decay constants of kaon and D-mesons from $N_{\rm f} = 2$ twisted mass lattice QCD," JHEP **0907**, 043 (2009) [arXiv:0904.0954 [hep-lat]].

[8] **ETM** Collaboration, V. Bertone *et al.*, "Kaon oscillations in the Standard Model and Beyond using $N_{\rm f} = 2$ dynamical quarks," PoS **LAT2009** (2009) 258. [arXiv:0910.4838 [hep-lat]].

[9] **ETM** Collaboration, B. Blossier *et al.*, "A proposal for B-physics on current lattices," arXiv:0909.3187 [hep-lat].

[10] **ETM** Collaboration, B. Blossier *et al.*, "f_B and f_{B_s} with maximally twisted Wilson fermions," [arXiv:0911.3757 [hep-lat]].

[11] **ETM** Collaboration, K. Jansen, C. Michael, A. Shindler and M. Wagner, "The Static-light meson spectrum from twisted mass lattice QCD," JHEP **0812**, 058 (2008) [arXiv:0810.1843 [hep-lat]].

[12] **ETM** Collaboration, C. Michael, A. Shindler and M. Wagner, "The continuum limit of the static-light meson spectrum," arXiv:1004.4235 [hep-lat].

[13] **ETM** Collaboration, B. Blossier, M. Wagner and O. Pène, "Lattice calculation of the Isgur-Wise functions $\tau_{1/2}$ and $\tau_{3/2}$ with dynamical quarks," JHEP **0906**, 022 (2009) [arXiv:0903.2298 [hep-lat]].

[14] **ETM** Collaboration, R. Frezzotti, V. Lubicz and S. Simula, "Electromagnetic form factor of the pion from twisted-mass lattice QCD at $N_{\rm f} = 2$," Phys. Rev. D **79**, 074506 (2009) [arXiv:0812.4042 [hep-lat]].

[15] **ETM** Collaboration, V. Lubicz, F. Mescia, S. Simula *et al.*, "$K \to \pi\ell\nu$ semileptonic form factors from two-flavor lattice QCD," Phys. Rev. **D80** (2009) 111502. [arXiv:0906.4728 [hep-lat]].

[16] **ETM** Collaboration, S. Di Vita *et al.*, "Vector and scalar form factors for K- and D-meson semileptonic decays from twisted mass fermions with $N_{\rm f} = 2$," PoS **LAT2009** (2009) 257. [arXiv:0910.4845 [hep-lat]].

[17] **ETM** Collaboration, C. Alexandrou *et al.*, "Nucleon form factors with dynamical twisted mass fermions," PoS **LATTICE2008**, 139 (2008) [arXiv:0811.0724 [hep-lat]].

[18] **ETM** Collaboration, R. Baron, S. Capitani, J. Carbonell, K. Jansen, Z. Liu, O. Pene and C. Urbach, "Moments of meson distribution functions with dynamical twisted mass fermions," PoS **LAT2007**, 153 (2007) [arXiv:0710.1580 [hep-lat]].

[19] **ETM** Collaboration, C. Michael and C. Urbach, "Neutral mesons and disconnected diagrams in twisted mass QCD," PoS **LAT2007**, 122 (2007) [arXiv:0709.4564 [hep-lat]].

[20] **ETM** Collaboration, K. Jansen, C. Michael and C. Urbach, "The η' meson from lattice QCD," Eur. Phys. J. C **58**, 261 (2008) [arXiv:0804.3871 [hep-lat]].

[21] **ETM** Collaboration, C. McNeile, C. Michael and C. Urbach, "The ω-ρ meson mass splitting and mixing from lattice QCD," Phys. Lett. B **674**, 286 (2009) [arXiv:0902.3897 [hep-lat]].

[22] **ETM** Collaboration, D. B. Renner and X. Feng, "Hadronic contribution to $g-2$ from twisted mass fermions," PoS **LATTICE2008**, 129 (2008) [arXiv:0902.2796 [hep-lat]].

[23] **ETM** Collaboration, X. Feng, K. Jansen and D. B. Renner, "The π^+ π^+ scattering length from maximally twisted mass lattice QCD," Phys. Lett. B **684**, 268 (2010) [arXiv:0909.3255 [hep-lat]].

[24] **ETM** Collaboration, X. Feng, K. Jansen and D. B. Renner, "Scattering from finite size methods in lattice QCD," arXiv:0910.4871 [hep-lat].

[25] **ETM** Collaboration, M. Constantinou *et al.*, "Non-perturbative renormalization of quark bilinear operators with $N_{\rm f} = 2$ (tmQCD) Wilson fermions and the tree-level improved gauge action," arXiv:1004.1115 [hep-lat].

[26] K. Cichy, J. Gonzalez Lopez, K. Jansen, A. Kujawa and A. Shindler, "Twisted mass, overlap and Creutz fermions: cut-off effects at tree-level of perturbation theory," Nucl. Phys. B **800**, 94 (2008) [arXiv:0802.3637 [hep-lat]].

[27] $\chi_{\rm L}$**F** Collaboration, K. Jansen, M. Papinutto, A. Shindler, C. Urbach and I. Wetzorke, "Light quarks with twisted mass fermions," Phys. Lett. B **619**, 184 (2005) [arXiv:hep-lat/0503031].

[28] $\chi_{\rm L}$**F** Collaboration, K. Jansen, M. Papinutto, A. Shindler, C. Urbach and I. Wetzorke, "Quenched scaling of Wilson twisted mass fermions," JHEP **0509**, 071 (2005) [arXiv:hep-lat/0507010].

[29] A. M. Abdel-Rehim, R. Lewis and R. M. Woloshyn, "Spectrum of quenched twisted mass lattice QCD at maximal twist," Phys. Rev. D **71**, 094505 (2005) [arXiv:hep-lat/0503007].

[30] **ETM** Collaboration, C. Urbach, "Lattice QCD with two light Wilson quarks and maximally twisted mass," PoS **LAT2007** (2007) 022 [arXiv:0710.1517 [hep-lat]].

[31] **ETM** Collaboration, P. Dimopoulos, R. Frezzotti, G. Herdoiza, C. Urbach and U. Wenger, "Scaling and low energy constants in lattice QCD with $N_{\rm f} = 2$ maximally twisted Wilson quarks," PoS **LAT2007** (2007) 102 [arXiv:0710.2498 [hep-lat]].

[32] R. Frezzotti, G. Martinelli, M. Papinutto and G. C. Rossi, "Reducing cutoff effects in maximally twisted lattice QCD close to the chiral limit," JHEP **0604** 038 (2006) [arXiv:hep-lat/0503034].

[33] **ETM** Collaboration, P. Dimopoulos, R. Frezzotti, C. Michael, G. C. Rossi and C. Urbach, "$\mathcal{O}(a^2)$ cutoff effects in lattice Wilson fermion simulations," Phys. Rev. D **81**, 034509 (2010) [arXiv:0908.0451 [hep-lat]].

[34] R. Frezzotti and G. C. Rossi, "Chirally improving Wilson fermions. II: Four-quark operators," JHEP **0410** (2004) 070 [arXiv:hep-lat/0407002].

[35] T. Chiarappa *et al.*, "Numerical simulation of QCD with u, d, s and c quarks in the twisted-mass Wilson formulation," Eur. Phys. J. C **50**, 373 (2007) [arXiv:hep-lat/0606011].

[36] **ETM** Collaboration, R. Baron *et al.*, "Status of ETMC simulations with $N_{\rm f} = 2 + 1 + 1$ twisted mass fermions," PoS **LATTICE2008**, 094 (2008) [arXiv:0810.3807 [hep-lat]].

[37] **ETM** Collaboration, R. Baron *et al.*, "First results of ETMC simulations with $N_{\rm f} = 2{+}1{+}1$ maximally twisted mass fermions," arXiv:0911.5244 [hep-lat].

[38] **ETM** Collaboration, R. Baron *et al.*, "Light hadrons from lattice QCD with light (u, d), strange and charm dynamical quarks", arXiv:1004.5284 [hep-lat].

[39] **MILC** Collaboration, A. Bazavov *et al.*, "HISQ action in dynamical simulations," PoS **LATTICE2008** (2008) 033 [arXiv:0903.0874 [hep-lat]].

[40] **MILC** Collaboration, A. Bazavov *et al.*, "Progress on four flavor QCD with the HISQ action," PoS **LAT2009** (2009) 123 [arXiv:0911.0869 [hep-lat]].

[41] **MILC** Collaboration, A. Bazavov *et al.*, "Scaling studies of QCD with the dynamical HISQ action," [arXiv:1004.0342 [hep-lat]].

[42] C. Pena, S. Sint and A. Vladikas, "Twisted mass QCD and lattice approaches to the Delta(I) = 1/2 rule," JHEP **0409** (2004) 069 [arXiv:hep-lat/0405028].

[43] A. M. Abdel-Rehim, R. Lewis, R. M. Woloshyn and J. M. S. Wu, "Strange quarks in quenched twisted mass lattice QCD," Phys. Rev. D **74** (2006) 014507 [arXiv:hep-lat/0601036].

[44] Y. Iwasaki, "Renormalization group analysis of lattice theories and improved lattice action: two-dimensional non-linear $\mathcal{O}(N)$ sigma model," Nucl. Phys. B **258**, 141 (1985).

[45] **ALPHA** Collaboration, R. Frezzotti, P. A. Grassi, S. Sint and P. Weisz, "Lattice QCD with a chirally twisted mass term," JHEP **0108**, 058 (2001) [arXiv:hep-lat/0101001].

[46] R. Frezzotti and G. C. Rossi, "Twisted-mass lattice QCD with mass non-degenerate quarks," Nucl. Phys. Proc. Suppl. **128** (2004) 193 [arXiv:hep-lat/0311008].

[47] R. Frezzotti and G. C. Rossi, "Chirally improving Wilson fermions. I: $\mathcal{O}(a)$ improvement," JHEP **0408**, 007 (2004) [arXiv:hep-lat/0306014].

[48] C. Amsler *et al.* [Particle Data Group], Phys. LettḂ **667**, 1 (2008) and 2009 partial update for the 2010 edition.

[49] **ALPHA** Collaboration, B. Blossier, M. Della Morte, G. von Hippel, T. Mendes and R. Sommer, "On the generalized eigenvalue method for energies and matrix elements in lattice field theory," JHEP **0904**, 094 (2009) [arXiv:0902.1265 [hep-lat]].

[50] **ALPHA** Collaboration, U. Wolff, "Monte Carlo errors with less errors," Comput. Phys. Commun. **156**, 143 (2004) [Erratum-ibid. **176**, 383 (2007)] [arXiv:hep-lat/0306017].

[51] C. Michael, "Fitting correlated data," Phys. Rev. D **49**, 2616 (1994) [arXiv:hep-lat/9310026].

[52] C. Michael and A. McKerrell, "Fitting Correlated Hadron Mass Spectrum Data," Phys. Rev. D **51**, 3745 (1995) [arXiv:hep-lat/9412087].

[53] F. Farchioni *et al.*, "Exploring the phase structure of lattice QCD with twisted mass quarks," Nucl. Phys. Proc. Suppl. **140**, 240 (2005) [arXiv:hep-lat/0409098].

[54] F. Farchioni *et al.*, "The phase structure of lattice QCD with Wilson quarks and renormalization group improved gluons," Eur. Phys. J. C **42**, 73 (2005) [arXiv:hep-lat/0410031].

[55] F. Farchioni *et al.*, "Numerical simulations with two flavours of twisted-mass Wilson quarks and DBW2 gauge action," Eur. Phys. J. C **47**, 453 (2006) [arXiv:hep-lat/0512017].

[56] R. Frezzotti, private communication (2008).